November 2023

POSITIVE FACTORIZATIONS VIA PLANAR MAPPING CLASSES AND BRAIDS

Richard E. Buckman
University of Massachusetts Amherst

POSITIVE FACTORIZATIONS VIA PLANAR MAPPING CLASSES AND BRAIDS

A Dissertation Presented

by

RICHARD E. BUCKMAN

Submitted to the Graduate School of the
University of Massachusetts Amherst in partial fulfillment
of the requirements for the degree of

DOCTOR OF PHILOSOPHY

September 2023

Mathematics & Statistics

POSITIVE FACTORIZATIONS VIA PLANAR MAPPING CLASSES AND BRAIDS

A Dissertation Presented

by

RICHARD E. BUCKMAN

Approved as to style and content by:

R. İnanç Baykur, Chair

Weimin Chen, Member

Noriyuki Hamada, Member

Ben Heidenreich, Member

Robin C. Young, Department Head
Mathematics & Statistics

DEDICATION

Dedicated to my daughter Julianne,

with blanket dedication to Kissie, her (not-just-a-) blanket,

to my most beautiful wife Dana Alhaffar,

to my mother Diane Gilleece,

and to my father Richard E. Buckman, in loving memory.

ACKNOWLEDGMENTS

I extend heartfelt thanks to my advisor, İnanç Baykur, and my committee members, Noriyuki Hamada, Weimin Chen, and Ben Heidenreich. I'm also deeply grateful to many other advisors-in-spirit, including Lori Goldner, Robert Kusner, Tom Braden, Jennie Traschen, David Kastor, and Narayanan Menon.

Most of all, I am grateful to my wife, Dana, and my daughter, Julianne, for their love and support, and to my mother and father, Diane Gilleece and Richard E Buckman, to whom I owe my passion, drive, confidence, and dedication.

I'm particularly grateful to Ilona Trousdale for help finding my way, from being lost at the ground floor because all the rooms had been renumbered, to being lost on the top floor, because all the rooms have been renumbered; Hans Johnston for the magnetic Hagoromo eraser; A. Havens for invading my first office, being a math conspirator, and introducing me to İnanç and Kirby calculus; Jason McGibbon for encouraging me to go to graduate school, inspiring me back to mathematics, but most importantly teaching me to drive a manual and then selling me his stickshift; Joshua Gay for leading me to Amherst; Thomas Mclennan for keen dry commentary and help writing; Kristin Lieber, Daniel Nichols, Emmet Troxel, and Lee Walsh for reminding me to have fun with puzzles; Diane Bowman, for sharing her puzzles and then selling them to me; Lee and Maritza for selling me their stickshift; Joseph Ricker for running the Happy Valley Guitar Orchestra, for teaching me to appreciate the sound of his guitars, then selling them to me; Benjamin Gamari for insisting I use Python until insisting I use Haskell; Laura Dietz for generosity, encouragement, and letting me borrow her stickshift; Mahmud Ahmadov and Pranjal for helpful companionship, coffee, and food; Matt Haskins, for cutting my hair, when it is clear that it has been

cut; Youssef and his family, for the warm welcome, the deliciously toroidal falafel, and for allowing me to write most of this thesis at the table in the corner; and Richard Harrington for the beautifully pointy wire sculpture that came to my defense.

I'm also indebted to many others professors, mentors, relatives, friends, and collaborators, including, but in no way limited to the following incompressible, provably not well-orderable set: Ibtisam and Nabil Alhaffar, Kinan Alhaffar, Peter Amstutz, Christopher Arsenault, Mark Arsenault, Stewart Ascher, Joseph Babcock, Steven Baisden, Catherine Benincasa, Peter Blanchette, Guy Blaylock, Adam Blomberg, Allen Bonde, Michael Borotko, Alan Boulanger, Dale Buckman, Susan Buckman, Debbie Buckman, Louis Buckman, Cyrus Burt, Garret Cahill, Adena Calden, Eduardo Cattani, Dong Chen, Haskell Cohen, Thurlow Cook, John Cooper, Maria Correia, Jennie D'Ambroise, Carlo Dallapiccola, Maria Dascălu, Benny Davidovitch, Larry Davidson, Tori Day, Alex Dingle, Tony Dinsmore, Bob Dow, Patrick Dragon, Filip Dul, Richard Ellis, Tom Evans, Micah Feldman, Teddy Feldman, Phillip de Fremery, Adina Gianelli, Vicki Gilbert, Eugene Golowich, Stephen Gustin, Paul Hacking, Kaori Hamada, Sean Hart, Christopher Hocker, Christine Horn, Marsha Johnson, Yasin Karacan, David Kawall, Alex Kiriakopoulos, Jane Knapp, Eric Knyt, Medhat Korna, Robin Koytcheff, Krishna Kumar, Jacob Lagerstrom, Peter Laurent, Jinguo Lian, Travis Lowe, Eyal Markman, William Meeks, Jean Merritt, Peker Milas, Karen Modestino, Trevor Morris, Terry Mullen, Andrea Nahmod, Kai Nakamura, Maria Nikolaou, Peter Norman, Kaitlin O'Konis, Alexei Oblomkov, Steven Olson, Eric Osman, Jacob Oyer, Franz Pedit, Emrah Pektas, Ken Pollard, Matthew Pollock, Nikolay Prokof'ev, Annie Raymond, Luc Rey-Bellet, Michael Rice, Mark Ricker, Rudy Rucker, Nick Schmitt, Jerry Schurink, Hadeer El Samaloty, Ginalaurisa Shea, Hamidezra Shojaei, Sorbo, Megan Staples, Mike Sullivan, Nathan Sunukjian, Tom Weston, Nathaniel Whitaker, Sarah Willor, and Robin Young.

ABSTRACT

POSITIVE FACTORIZATIONS VIA PLANAR MAPPING CLASSES AND BRAIDS

SEPTEMBER 2023

RICHARD E. BUCKMAN

B.Sc. Mathematics, UNIVERSITY OF MASSACHUSETTS AMHERST

B.Sc. Physics, UNIVERSITY OF MASSACHUSETTS AMHERST

B.Sc. Computer Science, UNIVERSITY OF MASSACHUSETTS AMHERST

M.Sc. Physics, UNIVERSITY OF MASSACHUSETTS AMHERST

M.Sc. Mathematics, UNIVERSITY OF MASSACHUSETTS AMHERST

Ph.D., UNIVERSITY OF MASSACHUSETTS AMHERST

Directed by: Professor R. İnanç Baykur

In this thesis we seek to better understand the planar mapping class group in order to find factorizations of boundary multitwists, primarily to generate and study symplectic Lefschetz pencils by lifting these factorizations. Traditionally this method is applied to a disk or sphere with marked points, utilizing factorizations in the standard and spherical braid groups, whereas in our work we allow for multiple boundary components. Dehn twists along these boundaries give rise to exceptional sections of Lefschetz fibrations over the 2–sphere, equivalently, to Lefschetz pencils with base points.

These methods are able to derive an array of known examples of Lefshetz fibrations while giving their maximal exceptional sections. In particular, a family of examples

we obtain, which recapture unpublished examples by Baykur, Hamada and Korkmaz, allows us to demonstrate that two well-known inequalities on the number of non-separating and separating vanishing cycles are in fact sharp for every genus $g \geq 2$.

TABLE OF CONTENTS

LIST OF FIGURES

Figure **Page**

CHAPTER 1

INTRODUCTION

In this thesis, we study the planar mapping class group to better understand it and develop methods to find planar factorizations of boundary multitwists. We primarily apply them to study symplectic Lefschetz fibrations and pencils by lifting them to higher genus surfaces using Birman-Hilden theory. Each factorization determines a Lefschetz fibration, and each boundary corresponds to a section where the power of the Dehn twist along gives the self-intersection of this surface in the ambient oriented 4–manifold. In particular, when the boundary multitwist has a single power, these are exceptional sections corresponding to the base points of a Lefschetz pencil.

Donaldson showed that every symplectic 4-manifold admits a Lefschetz pencil with symplectic fibers which can be blown up to get a Lefschetz fibration [Don99]. Conversely, Gompf showed that the total space of a nontrivial Lefschetz fibration admits a symplectic structure [GS99]. Therefore, finding Lefschetz fibrations and/or supporting Lefschetz pencils through positive factorizations give a combinatorial way to discover new examples of symplectic 4-manifolds.

Given a genus g surface S without boundary, and a product of ℓ positive Dehn twists in the mapping class group $\mathrm{Mod}(S)$ that give a factorization of the identity, we can construct a Lefschetz fibration over a sphere with ℓ singular points. If instead, S has boundary, then given a positive factorization of the boundary multitwist with one positive boundary twist for each boundary component, we can fill in the boundaries to get a Lefschetz fibration with a (-1)–section where each boundary component was. These can be blown down to get a Lefschetz pencil.

We can apply a slightly generalized version of Birman-Hilden theory to lift factorizations of the planar mapping class group with marked points to factorizations of our higher genus mapping class groups with boundaries to obtain Lefschetz fibrations with a symmetry, which is induced by a certain involution (a hyperelliptic involution, when the boundaries are capped off) on the fibers. We develop diagrammatic methods to build such examples, in order to get new (positive) factorizations in the planar mapping class group to generate interesting Lefschetz fibrations and pencils.

Organization:

Here in Chapter 1, we give a brief introduction and outline.

In Chapter 2 we give an overview of some background material, including symplectic 4–manifolds, Lefschetz fibrations and pencils, and mapping class groups of surfaces.

In Chapter 3 we describe our diagrams for factorizations of planar mapping classes. First, we show that in the context of planar mapping class factorizations, we can use an invariant that effectively allows us to describe planar mapping classes as elements of the standard braid group with integral weights, leading to a variation of braid diagrams. Then we discuss some elementary techniques and key examples used in the later chapters to derive more advanced examples.

In Chapter 4, by lifting factorizations of planar mapping classes, we derive an interesting family of Lefschetz pencils. After blowing up the base points, these yield genus–g Lefschetz fibrations $f_g\colon X_{\mathrm{BK}} \to S^2$ which generalize the genus $g = 2$ Lefschetz fibration of Baykur and Korkmaz [BK17].

Chapter 5 details how to calculate some of the homological invariants of the ambient 4–manifold such as its signature and the first homology, in preparation for our results in the last chapter.

Finally, in Chapter 6, we discuss —with proofs— a pair of inequalities on the number of non-separating and separating vanishing cycles of a Lefschetz fibration

over the 2–sphere, and then show using the examples $f_g \colon X_{\mathrm{BK}} \to S^2$ that these inequalities are in fact sharp. This constitutes the main result of our thesis.

CHAPTER 2

BACKGROUND

2.1 Symplectic 4-manifolds

A *topological n-manifold* M is a topological space locally homeomorphic to $\mathbb{R}^n$, required to be second-countable and Hausdorff. A *smooth manifold* $(M, \mathcal{A})$ pairs M with an additional *smooth structure* given by a maximal smooth atlas $\mathcal{A}$ providing local diffeomorphisms to $\mathbb{R}^n$.

The interplay between topological properties and smooth properties is surprisingly rich and complex, especially so for 4-manifolds. For example, two smooth manifolds form an *exotic pair* when they are homeomorphic but not diffeomorphic, and a manifold M which forms an exotic pair with a sphere S^n or a euclidean space $\mathbb{R}^n$ is often referred to as an exotic S^n or an exotic $\mathbb{R}^n$. Stallings showed that there are no exotic pairs involving $\mathbb{R}^n$ for $n \neq 4$ [Sta62], but following the work of Freedman and Donaldson, many examples were discovered examples for $n = 4$. In fact Taubes discovered not only infinitely many, but an uncountable continuum. Understanding this and other related phenomena leads us to the study of 4-manifolds in particular, and the many related subclasses of manifolds surrounding them, including symplectic manifolds, along with Lefschetz fibrations and pencils.

On an n-dimensional vector space V over $\mathbb{R}$, a bilinear map $\Omega : V \times V \to \mathbb{R}$ is *skew-symmetric* when $\Omega(u, v) = -\Omega(v, u)$ for all $u, v \in V$. A skew-symmetric bilinear map Ω is *nondegenerate* if whenever $\Omega(u, v) = 0$ for all $v \in V$, then $u = 0$. Then we call Ω a *symplectic structure* on V and the pair (V, Ω) is a *symplectic vector space*.

$\Omega^k(M)$ denotes the set of real differential k-forms on M, with exterior derivative $d : \Omega^k(M) \to \Omega^{k+1}(M)$. Given $\omega \in \Omega^k(M)$, we say ω is *closed* when $d\omega = 0$.

At each $p \in M$, a 2-form $\omega \in \Omega^2(M)$ defines $\omega_p : T_pM \times T_pM \to \mathbb{R}$, a skew-symmetric bilinear map on the tangent space at p, and ω_p varies smoothly over p. We say that ω is *symplectic* when it is closed and non-degenerate, implying that (T_pM, ω_p) defines a symplectic vector space for each $p \in M$. Then the pair (M, ω) defines a *symplectic manifold* which must be even dimensional. In fact, a classical theorem of Darboux tells us that every symplectic manifold has local coordinate charts $(x_1, \ldots, x_n, y_1, \ldots, y_n)$ where ω is given by $\Sigma_{i=1}^n dx_i \wedge dy_i$.

2.2 Lefschetz fibrations and pencils

Lefschetz fibrations generalize fiber bundles, further generalizing product spaces, establishing higher dimensional spaces as combinations of lower dimensional spaces. In this thesis we are primarily interested in Lefschetz fibrations in 4 dimensions over a 2-sphere, omitting both higher dimensions and other possible base spaces.

As in [GS99], we define a 4 dimensional *Lefschetz fibration* as a singular map $f\colon X \to \Sigma$ from a 4-manifold X to the 2-manifold Σ with finite critical point set P, requiring each critical point to have a neighborhood with local complex coordinates (compatible with the orientation on X) where f is given by $f(z_1, z_2) = z_1^2 + z_2^2$. We assume that f is injective on its critical set. The fiber $F_p \subset X$ above any point $p \in \Sigma$ denotes the preimage of p under f. Let $q_i := f(p_i)$ denote the critical values and choose any regular value $q_0 \in \Sigma$ to define the regular fiber $F := F_{q_0} \cong \Sigma_g$, where g defines the genus of our Lefschetz fibration. For any regular value $p \in \Sigma$ we have $F_p \cong F$, but any singular value $p = q_i$, F_p has a *singular fiber* with associated *vanishing cycle* $c_i \subset \Sigma_g$, an essential simple closed curve that gets pinched to a point making F_p a surface with a single double-point (*node*) singularity. The local monodromy around q_i is known to be a Dehn twist t_{c_i} in the mapping class group

$\mathrm{Mod}(\Sigma_g)$. In fact, by [Kas80], a handlebody decomposition for the manifold X can be obtained by starting with the trivial fiber bundle $\Sigma_g \times D^2$ and attaching 2-handles along the vanishing cycles with -1 framing with respect to the fiber. The union of this with another copy of $\Sigma_g \times D^2$ then gives X. (Or equivalently, by one more 2–handle attachment to the former piece, followed by $2g$ 3– and a single 4– handle attachment.)

When the base surface is a 2-sphere, we can think of it as two disks glued together, one disk containing all the critical values, together with a regular value q_0. Pick pairwise non-intersecting (except at q_0) simple closed paths γ_i based at q_0, enclosing q_i (in this disk), running counterclockwise. The local monodromy over γ_i would be the Dehn twist t_{c_i}, where now all these local monodromies can be expressed in the mapping class group of the same reference regular fiber $F = F_{q_0}$. Then the monodromy over a simple closed path homotopic to the concatenation of the paths $\gamma_1, \ldots, \gamma_\ell$ factorizes into the product $t_{c_\ell} \cdots t_{c_2} t_{c_1}$. Since the fibration over the other disk is trivial, this is a factorization of identity in the mapping class group of $F \cong \Sigma_g$.

Thus genus–g Lefschetz fibrations over a sphere correspond to positive factorizations of the identity in the mapping class group of a genus g surface Σ_g, precisely the reason we are interested in finding such factorizations.

A Lefschetz fibration is *hyperelliptic* when each of its vanishing cycles is invariant under a fixed hyperelliptic involution of the regular fiber. We also introduce a subtle distinction by saying a Lefschetz fibration is *symmetric* when the monodromy factorization has a factor $t_a t_b$ along a pair of symmetric curves a and b mapped to each other under the hyperelliptic involution; this element represents a mapping class commuting with the hyperelliptic involution.

A *Lefschetz pencil* on a 4-manifold X is defined by a finite nonempty base point set $B \subset X$ and a singular function $f\colon X \setminus B \to S^2$ with finite non-empty critical set $P \subset X$, requiring local complex coordinates around each base point $b \in B$ such

that f is given by the projectivization $\mathbb{C}^2 - \{0\} \to \mathbb{CP}^1 \cong S^2$, in local coordinates $(z_1, z_2) \to z_1/z_2$, and requiring each critical point $p \in P$ to be of nodal type.

Given a Lefschetz pencil, blowing up each of the base points consecutively results in a Lefschetz fibration over S^2 with a -1 section from each exceptional sphere. Given a Lefschetz fibration over S^2 with a set of -1 sections, we can blow-down each of the sections to get a Lefschetz pencil with corresponding base points.

2.3 Mapping class groups of surfaces

Surfaces. We consider a surface (denoted by S, generically) to be compact, connected, and oriented, possibly with boundary ∂S. In particular, $\Sigma_{g,n}^b$ specifies a compact oriented genus g surface with b boundary components (often shortened to boundaries) and n marked points in the interior.

A surface is *planar* when it has genus zero and nonempty boundary, i.e. when it can be embedded in $\mathbb{R}^2$. Thus, a sphere (denoted by $\mathbb{S}_n$, with n marked points or $\mathbb{S}$, when unmarked) is not planar but a disk ($\mathbb{D}_n$ with marked points or $\mathbb{D}$ unmarked) is. A sphere with $b+1$ disjoint open disks removed ($\mathbb{S}_n^{b+1}$) becomes planar, equivalent to a disk with b disjoint open disks removed ($\mathbb{D}_n^b$). In particular, for planar surfaces, we use the terms sphere and disk interchangeably, and they still apply when there are additional boundary components. We tend to use the term sphere when we would imagine the surface sitting in $\mathbb{R}^3$ where the boundaries are indistinguishable, while we tend to use the term disk when we would imagine the surface in $\mathbb{R}^2$ where one boundary is (superficially) distinguished as the *"exterior" boundary*. In the latter case, we use δ_0 to refer to the exterior boundary, with *interior boundaries* $\{\delta_1, \ldots, \delta_b\}$. This will be the default for most of this thesis, since it is more convenient to draw diagrams and manipulate them using disks. Most important, we define an invariant which fits with a diagram as drawn on a disk and depends on having the exterior boundary to give a well defined inside and outside to closed curves. Still, when we

are lifting them to higher genus surfaces, it is more convenient to relate the different surfaces using spheres.

Higher genus surfaces are drawn as we would see them if embedded in $\mathbb{R}^3$, but planar surfaces will only be drawn this way to relate them to higher genus surfaces. Most of the time they will be drawn as embedded in $\mathbb{R}^2$. In this case, since we are usually thinking of the surface as a disk $\mathbb{D}_n^b$, we omit the exterior boundary for aesthetics and ease of drawing, essentially using the edge of the diagram in its place. Other times we think of the same surface as a sphere $\mathbb{S}_n^{b+1}$, which looks identical, except that all the boundaries are drawn identically, with the edge of the diagram only artificial, so that the sphere extends around behind the paper, essentially gluing an unmarked disk to it. This is more symmetric and treats all boundaries as equivalent, but one needs to recall that we can also isotope curves around the sphere. Note that this introduces a potential ambiguity since a diagram of $\mathbb{D}_n^b$ with implicit exterior boundary is indistinguishable from the diagram of $\mathbb{S}_n^{b-1}$, but we will clearly indicate the difference.

We represent marked points using blue dots, and boundaries using grey dots. For uniformity, we will typically arrange the points in a horizontal row, with marked points on the left and boundaries to the right, unless there is a reason to use other arrangements. Higher genus surfaces considered in this thesis will not have marked points.

On a given surface S, we consider a *curve* to be a simple closed curve embedded in S, avoiding marked points or boundaries, up to isotopies also avoiding marked points (and fixing boundaries pointwise). Similarly, we consider an *arc* to be a simple proper arc embedded in S, with distinct endpoints each given by either a marked point or a boundary point, otherwise avoiding marked points and boundaries, up to isotopies fixing the marked points and boundaries. We assume that all intersections between arcs and/or curves are transverse, with at most double-points.

A closed curve $c \subset S$ is a *separating* curve if $S \setminus c$ has two disjoint components. Every closed curve on a planar surface is separating.

On a disk, we say that a given boundary or marked point is *inside* a curve c when it is not on the same component of $S \setminus c$ that contains the exterior boundary δ_0. On a sphere, there is no well-defined "inside" without choosing an exterior boundary.

Given a boundary δ_i, we say the component of $S \setminus c$ which contains δ_i is *outside* c *relative to* δ_i, and the other component is *inside* c *relative to* δ_i, extending the terminology to the marked points or boundaries contained in each component.

On a planar diagram, marked points or boundaries are drawn inside a curve c precisely when they are inside c relative to the exterior boundary δ_0. On a spherical diagram, this is not necessarily true since isotoping c around the sphere will turn c inside out, exchanging what is drawn inside or outside.

Mapping class groups. We now discuss mapping class groups. Given a pair (S, Δ) with surface S and $\Delta \subset S$, define $\mathrm{Homeo}^+(S, \Delta)$ as the group of orientation preserving homeomorphisms on S that preserve Δ pointwise and the marked point set setwise, endowed with the compact-open topology [FM12]. We then define the *mapping class group* $\mathrm{Mod}(S) = \pi_0(\mathrm{Homeo}^+(S, \partial S))$ and the related *relative mapping class group* on a pair (S, Δ) as $\mathrm{Mod}(S, \Delta) = \pi_0(\mathrm{Homeo}^+(S, \partial S \cup \Delta))$.

Every mapping class group is generated by a combination of Dehn twists and arc half-twists, here considered to be positive when right-handed (as opposed to [FM12]). A simple closed curve $c \subset S$ avoiding marked points or boundaries corresponds to a *Dehn twist* t_c, while an *arc half-twist* τ_α corresponds to a simple proper arc $\alpha \subset S$ with endpoints given by distinct marked points but similarly avoiding marked points or boundaries otherwise. We refer to a Dehn twist t_c as a *boundary Dehn twist* if c is parallel to a boundary δ_i, referring to it as t_{δ_i} even though c is not actually δ_i.

The *boundary multitwist* is the product of all boundary Dehn twists, i.e. $t_{\delta_b} t_{\delta_{b-1}} \cdots t_{\delta_0}$ when there are $b+1$ boundaries with any number of marked points.

In diagrams, we notate a Dehn twist t_c or an arc half-twist τ_α with c or α, using magenta for positive twists and green for inverse twists, optionally using an adjacent number to indicate that the twist is raised to a power. The mapping class group is most directly understood by considering the actions of mapping classes on a combination of simple closed curves and simple proper arcs with endpoints between either marked points or boundaries.

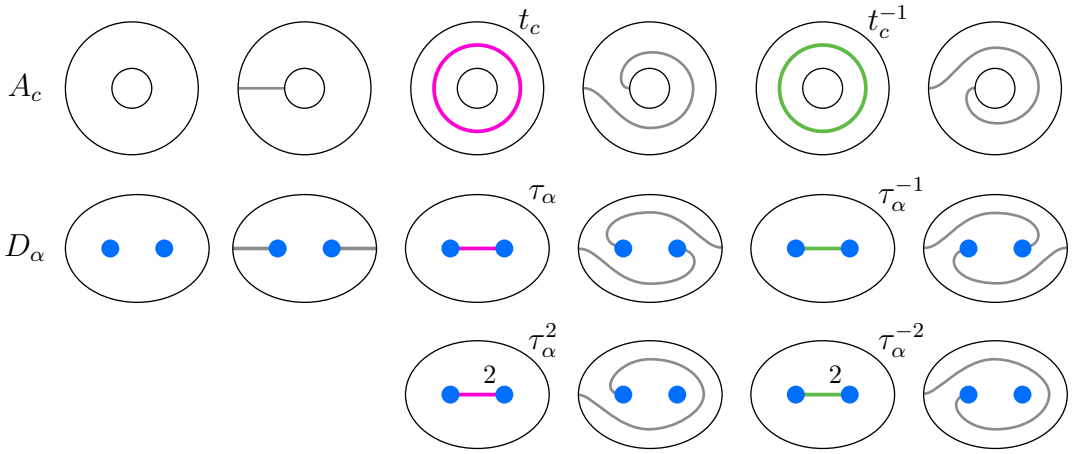

Figure 2.1. Top: The action of a Dehn twist t_c is restricted to a neighborhood A_c of c, an annulus drawn as $\mathbb{D}^1$. Middle: The action of an arc half-twist τ_α is restricted to a neighborhood D_α of α, drawn as a disk $\mathbb{D}_2$ with two marked points. Bottom: The action of an arc half-twist squared τ_α^2 is equivalent to the action of the Dehn twist around a curve parallel to the boundary of the disk neighborhood.

The action of a Dehn twist t_c or its inverse can be understood locally in a neighborhood A_c of c, an annulus ($\cong \mathbb{D}^1$). Any simple closed curve or simple proper arc can be isotoped to intersect A_c at a (possibly empty) set of disjoint arcs, each between the distinct boundaries of A_c and intersecting c once, as seen in the top row in the second column of Figure 2.1. Then t_c replaces each of these arcs with a right-veering arc around the annulus as seen in the fourth column, and the inverse t_c^{-1} replaces each with a left-veering arc around the annulus seen in the sixth column, while leaving portions outside A_c untouched in either case.

The action of an arc half-twist τ_α can be understood locally in a disk neighborhood D_α of α with the two marked points, the end points of α ($\cong \mathbb{D}_2$). Any simple closed curve or simple proper arc (which is not isotopic to α) away from its endpoints can be isotoped to intersect D_α at a (possibly empty) set of disjoint arcs, each between the top of D_α to the bottom, intersecting α once. This is not drawn in Figure 2.1, but is the only possible arc connecting the top and bottom of D_α in the second column without intersecting either arc segment. In all cases, the action of τ_α or its inverse on D_α can be seen in the fourth and sixth columns, as the only possible arc connecting the top or bottom, or as one of the two resulting arcs shown, exchanging the marked points. A proper arc that is isotopic to α stays the same, although it is going in the opposite direction if oriented since the marked points are exchanged.

2.4 Birman-Hilden theory

Here we introduce Birman-Hilden theory, but only as needed to establish the necessary terminology and conventions we use. A more detailed introduction can be found in [MW21] and [FM12].

Basic setup. Suppose Σ_g sits in $\mathbb{R}^3$ as in Figure 2.2 so that it is symmetric with respect to the π rotation around the dotted horizontal axis. Let $\iota : \Sigma_g \to \Sigma_g$ be the *hyperelliptic involution*, which is induced from the π rotation. Then taking the quotient by ι forms the *Birman-Hilden double branched cover* $p : \Sigma_g \to \Sigma_g/\iota = \mathbb{S}_{2g+2}$, which maps fixed points of ι to marked points of $\mathbb{S}_{2g+2}$. (Here we find it convenient to denote the base with the branched points.) We fix $g+1$ branch cuts as in Figure 2.2.

Let $S \subset \mathbb{S}_{2g+2}$ be the closed surface, possibly with marked points, resulting from the removal of a nonempty finite union of disjoint open disks from $\mathbb{S}_{2g+2}$, where each disk is either unmarked or singly marked. Let $\widetilde{S} = p^{-1}(S) \subset \Sigma_g$ be the closed surface lifting S with respect to p, so that restricting p to $\widetilde{S}$ is also a double cover, branched unless there are no marked points remaining in S. We allow ι and p to also refer

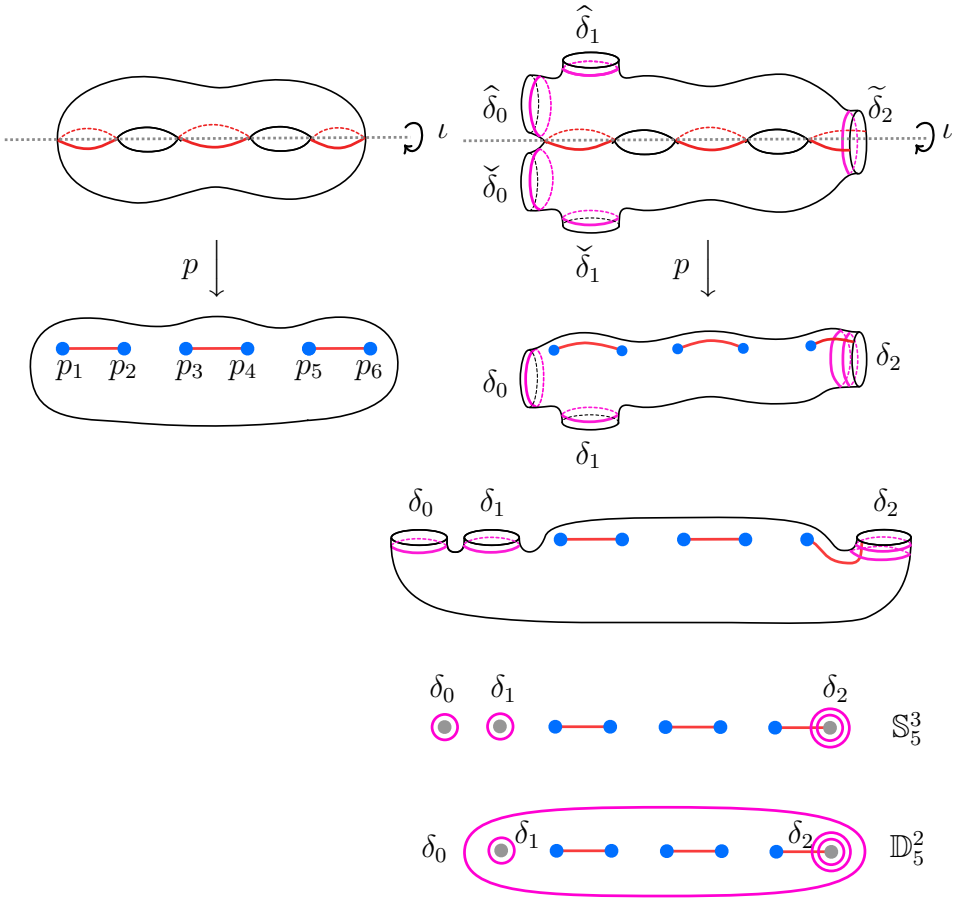

Figure 2.2. Left: Σ_2 with the hyperelliptic involution ι giving the Birman-Hilden double cover of $\mathbb{S}_6$. Right: A branched boundary and 2 unbranched boundaries on $\mathbb{S}^3_5$ give Σ^5_2 with involution ι giving a double cover of $\mathbb{S}^3_5$, or equivalently, $\mathbb{D}^2_5$.

to the restricted maps $\iota\colon \widetilde{S} \to \widetilde{S}$ and $p\colon \widetilde{S} \to S$. The horizontal plane through the dotted line cuts $\widetilde{S}$ into the upper half and lower half subsurfaces $\widehat{S}, \check{S} \subset \widetilde{S}$, which are referred to as the *upper* and *lower sheets*. Both $\widehat{S}$ and $\check{S}$ are homeomorphic to the complement of the branch cuts in S.

Lifting curves and arcs. We say a curve $c \subset S$ has *even parity* (or is an even parity curve) if it transversely intersects the branch cuts an even number of times, generically, and that c has *odd parity* (or is an odd parity curve) otherwise. By extension, we say a Dehn twist $t_c \in \mathrm{Mod}(S)$ has the same parity as c (or is an even or odd parity Dehn twist).

We say that a closed curve $c \subset \widetilde{S}$ is *symmetric* if ι fixes c setwise, and that a pair of disjoint closed curves $c_1, c_2 \subset \widetilde{S}$ is a *symmetric pair* if ι swaps c_1 and c_2. Again, we extend both terms to Dehn twists in $\mathrm{Mod}(\widetilde{S})$.

We note that $p : \widetilde{S} \to S$ projects (1) each nonseparating symmetric closed curve $a \subset \widetilde{S}$ to an arc α between marked points, (2) each separating symmetric closed curve $c \subset \widetilde{S}$ to a closed curve $\underline{c}$ with odd parity, and (3) each c_i in a symmetric pair $\{c_1, c_2\}$ of closed curves to a closed curve $\underline{c} = p(c_1) = p(c_2)$ with even parity. Conversely, any arc $\alpha \subset S$ between marked points lifts to a nonseparating symmetric closed curve $a \subset \widetilde{S}$. Similarly, any closed curve $c \subset S$ lifts to either a separating symmetric closed curve $\overline{c}$ or a symmetric pair $\{\hat{c}, \check{c}\}$ of closed curves depending on odd or even parity.

We also note that any closed curve $c \subset S$ is separating, and if c has even parity then the two components of $S \setminus c$ lift to disjoint components of $\widetilde{S} \setminus (\hat{c} \cup \check{c})$. This implies that any symmetric pair $\{\hat{c}, \check{c}\}$ of closed curves in $\widetilde{S}$ is separating, although neither curve is individually separating.

We use the naming conventions used here whenever possible to make it clearer how curves and arcs relate to each other. When possible, a hat ($\hat{\alpha}$ or $\hat{c}$) will be associated with the upper sheet and a check ($\check{\alpha}$ or $\check{c}$) will be associated with the lower sheet, but these often are not in a single sheet. A Greek letter will indicate an arc, so that $\check{\alpha}$ and $\hat{\alpha}$ would be two arcs with union a, and a Roman letter will indicate a closed curve.

Each boundary $\delta \subset S$ is a closed curve, so it has even or odd parity. In the odd case, we say δ is a *branched boundary*, and the lift $\widetilde{\delta} \subset \widetilde{S}$ is a *symmetric boundary*. In the even case, we say δ is an *unbranched boundary*, and the lifts $\widehat{\delta}, \check{\delta} \subset \widetilde{S}$ are a *symmetric pair of boundaries*. Without loss of generality we can assume that a branched boundary intersects a branch cut once and an unbranched boundary is disjoint from any branch cuts.

Let S have $b+1$ boundary components, $\{\delta_0, \ldots, \delta_b\}$, b_{I} of them branched and b_{II} of them unbranched. Each branched boundary δ_i lifts to the symmetric boundary $\widetilde{\delta}_i$, and each unbranched boundary δ_i lifts to a symmetric pair of boundaries $\widehat{\delta}_i$ and $\check{\delta}_i$ in the upper and lower sheets, so $\widetilde{S}$ has $b_{\mathrm{I}} + 2b_{\mathrm{II}}$ total boundary components. For $n := 2g + 2 - b_{\mathrm{I}}$ marked points in S, with $g \in \mathbb{N}$, we have $S \cong \mathbb{S}^{b+1}_n \cong \mathbb{D}^b_n$ and $\widetilde{S} \cong \Sigma_g^{b_{\mathrm{I}}+2b_{\mathrm{II}}}$.

Symmetric and liftable mapping class groups. We then define the *symmetric mapping class group* $\mathrm{SMod}(\widetilde{S}) \subset \mathrm{Mod}(\widetilde{S})$ as the group of elements $\phi \in \mathrm{Mod}(\widetilde{S})$ having fiber preserving representative maps $f : \widetilde{S} \to \widetilde{S}$, i.e. $\iota \circ f = f \circ \iota$, or equivalently $p \circ f = p$, and we define the *liftable mapping class group* $\mathrm{LMod}(S)$ as the group of elements $\phi \in \mathrm{Mod}(S)$ having representative maps $f : S \to S$ which lift to representative maps $\tilde{f} : \widetilde{S} \to \widetilde{S}$ of $\mathrm{Mod}(S)$, i.e. $f \circ p = p \circ \tilde{f}$.

Then p induces a map $\Phi : \mathrm{SMod}(\widetilde{S}) \to \mathrm{LMod}(S)$. Letting $\mathrm{Deck} \subset \mathrm{SMod}(\widetilde{S})$ be the subgroup of deck transformations fixing boundaries pointwise, we have an isomorphism $\mathrm{SMod}(\widetilde{S})/\mathrm{Deck} \cong \mathrm{LMod}(S)$. In our setup Φ is an isomorphism, and hence

$$\mathrm{SMod}(\widetilde{S}) \cong \mathrm{LMod}(S),$$

since the nonempty boundaries of S and $\widetilde{S}$ prevent ι from being a representative map, so that Deck is trivial.

Lifting Dehn twists and half-twists. Now, we list certain simple types of symmetric and liftable mapping classes that we will use in lifting factorizations in planar mapping class groups to ones in higher genera mapping class groups.

Elementary symmetric mapping classes:

1. Given a non-separating symmetric closed curve $a \subset \widetilde{S}$, we have $t_a \in \mathrm{SMod}(\widetilde{S})$ and $\Phi(t_a) = \tau_\alpha$ where $\alpha = p(a) \subset S$ is an arc between two marked points.

2. Given a separating symmetric closed curve $c \subset \widetilde{S}$, we have $t_c \in \mathrm{SMod}(\widetilde{S})$ and $\Phi(t_c) = t_{\underline{c}}^2$ where $\underline{c} = p(c) \subset S$ is an odd parity closed curve.

3. Given a symmetric pair of closed curves $c_1, c_2 \subset \widetilde{S}$, we have $t_{c_1} t_{c_2} \in \mathrm{SMod}(\widetilde{S})$ and $\Phi(t_{c_1} t_{c_2}) = t_{\underline{c}}$ where $\underline{c} = p(c_1) = p(c_2) \subset S$ is an even parity closed curve.

Since Φ is an isomorphism the converse is true as follows.

Elementary liftable mapping classes:

1. Given an arc $\alpha \subset S$ between marked points, we have $\tau_\alpha \in \mathrm{LMod}(S)$ and $\Phi^{-1}(\tau_\alpha) = t_a$ where $a = p^{-1}(\alpha) \subset \widetilde{S}$ is a non-separating symmetric closed curve.

2. Given an odd parity closed curve $c \subset S$, we have $t_c^2 \in \mathrm{LMod}(S)$ and $\Phi^{-1}(t_c^2) = t_{\overline{c}}$ where $\overline{c} = p^{-1}(c) \subset \widetilde{S}$ is a separating symmetric closed curve.

3. Given an even parity closed curve $c \subset S$, we have $t_c \in \mathrm{LMod}(S)$ and $\Phi^{-1}(t_c) = t_{\hat{c}} t_{\check{c}}$ where $\hat{c}, \check{c} \subset \widetilde{S}$ are a symmetric pair of closed curves such that $p^{-1}(c) = \hat{c} \cup \check{c}$.

In particular, if $\delta \subset S$ is a branched boundary then t_δ^2 lifts to $t_{\widetilde{\delta}}$ where $\widetilde{\delta} \subset \widetilde{S}$ is the corresponding symmetric boundary, while if $\delta \subset S$ is an unbranched boundary then t_δ lifts to $t_{\widehat{\delta}} t_{\check{\delta}}$ where $\widehat{\delta}, \check{\delta} \subset \widetilde{S}$ are the corresponding symmetric pair of boundaries.

CHAPTER 3

PLANAR FACTORIZATIONS

3.1 Diagrams of Factorizations

Factorizations. Let S be a planar surface with mapping class group $\mathrm{Mod}(S)$. A *positive twist* refers to either an arc half-twist τ_α or a single Dehn twist t_c, a *negative twist* refers to the inverse of a positive twist, and a *twist* refers to either. A word $\omega = \phi_\ell \cdots \phi_2 \phi_1$ is an ordered set of *factors* ϕ_i where each is a twist (or at times a square of Dehn twists when we focus on liftable factorizations) and the *product mapping class* of a word is the mapping class given by the product of the factors in order. A *factorization of the identity* is then a word with product mapping class equal to the identity, a *factorization of* ϕ is a word with product mapping class equal to ϕ, and a *relation* $\omega_1 = \omega_2$ is a pair of words with the same product mapping class.

Diagrams. The diagrams of factorizations we stumbled upon in this thesis seek to retain the powerfully intuitive sequential nature of braids while simplifying some of the inherent complexity in manipulating them.

Here we give an overview of the diagrams and the notations we use to manipulate them, although we hope that they have been refined enough that some familiarity with mapping class groups will make them almost immediate.

Compare the left half of Figure 3.2 to the left half of Figure 3.3 as it is represented using our diagrams. The factors in the diagram are given as rows of a column, with the top factor corresponding to the rightmost factor algebraically. The exception is that boundary twists can be freely expressed in the same row as there is no ambiguity in the order.

We start with the toy example in Figure 3.1 using $\mathbb{D}_3$, a disk with three marked points, so that the mapping class group $\mathrm{Mod}(\mathbb{D}_3)$ is equivalent to B_3, the 3–strand braid group.

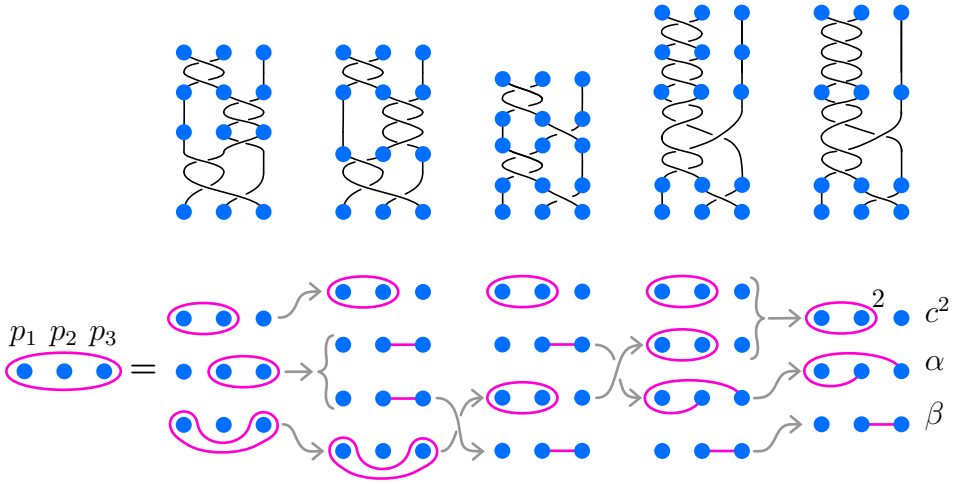

Figure 3.1. The reduced half lantern relation in $\mathrm{Mod}(\mathbb{D}_3)$ derived by starting with the reduced lantern relation in $\mathrm{Mod}(\mathbb{D}_3)$, underneath the corresponding derivation using the braid group B_3.

The first two columns with the equal sign between them indicate a relation, *the reduced lantern relation*, in this case. Otherwise, the arrows indicate the derivation from left to right, implying a relation between steps with justification given by the symbols. Braces indicating groupings are placed with arrows to indicate substitution is being made. The first step indicates that we are splitting the Dehn twist in the middle row into the two identical arc half-twists. Another simple substitution is shown in the fourth and final step where two identical Dehn twists are combined into a squared Dehn twist as a single factor. Substitutions other than splitting or combining, or cancelling pairs, will be made with more justification in the text.

Arrows without braces indicate *Hurwitz moves*. The arrow crossing over indicates the factor which acts on the other. If this factor moves down, the action is inverted, while it is applied directly if the factor moves up. For example, the second step here

moves the arc from the third position down to the fourth, moving the bottom Dehn twist up while acting inversely on it. The following step moves the Dehn twist up from the third position to the second position, moving the arc half-twist in the second position down to the third position, while acting positively on it.

The Hurwitz move notations combine into a braid which acts on the factors to perform arbitrarily long reorganizations, but we also allow the braids to intersect to indicate that the factors commute past each other, such as in the middle step of Figure 4.7 or the third step of Figure 4.8.

In Figure 4.7 in the first step, the long dashed arrow moving down, up behind the others, and down again is indicating a cyclic permutation that moves the bottom row to the top, always possible when the product mapping class is central as the squared boundary multitwist here is. In general this will require a global conjugation by the permuted elements, or a justification that they commute with the product mapping class.

Projection and reduced relations. Starting with $\mathbb{D}_n^b$, capping the interior boundaries $\{\delta_1, \delta_2, \ldots, \delta_b\}$ with singly marked disks with corresponding points $Q = \{p_1, \ldots, p_b\}$ induces a projection $\pi : \mathrm{Mod}(\mathbb{D}_n^b) \to \mathrm{Mod}(\mathbb{D}_{b+n}, Q)$, recalling that the target set here is the relative mapping class with respect to Q, the subgroup of $\mathrm{Mod}(\mathbb{D}_{b+n})$ whose elements fix the new marked points individually. The kernel K is generated by the interior boundary Dehn twists $t_{\delta_1}, t_{\delta_2}, \ldots, t_{\delta_b}$, since any curve parallel to δ_i now bounds a singly marked disk.

For the entirety of this thesis, we use π to refer to this map, often referred to as *the projection*.

Given any relation in $\mathrm{Mod}(\mathbb{D}_n^b)$, we can apply π to each side of the relation to get a corresponding relation we refer to as the *reduced relation* in $\mathrm{Mod}(\mathbb{D}_{b+n}, Q)$, or analogously, the reduced relation in $\mathrm{Mod}(\mathbb{D}_{b+n})$.

The above construction also applies to any subset of the boundaries with little difference, avoiding the details for clarity.

Examples of this can be seen throughout the thesis, but most notably in the diagrams introducing each of the relations in Section 3.4.

3.2 The Dehn twist invariant

The mapping class group $\mathrm{Mod}(\mathbb{D}_n)$ is isomorphic to the Artin braid group B_n, but the additional boundaries of $\mathbb{D}_n^b$ make $\mathrm{Mod}(\mathbb{D}_n^b)$ more complex. Applying the projection π reduces to a subgroup of $\mathrm{Mod}(\mathbb{D}_{n+b}) \cong B_{n+b}$, but not injectively. Despite this, the following invariant allows us to lift factorizations within $\mathrm{Mod}(\mathbb{D}_{n+b})$ to factorizations within $\mathrm{Mod}(\mathbb{D}_n^b)$.

We now define the invariant as a composition. We first apply the forgetful homomorphism

$$\mathit{Forget} : \mathrm{Mod}(\mathbb{D}_n^b) \to \mathrm{Mod}(\mathbb{D}^b),$$

which forgets the n marked points. Then for each boundary component δ_i, we use the capping homomorphism

$$\mathit{Cap}_{\delta_0,\delta_i} : \mathrm{Mod}(\mathbb{D}^b) \to \mathrm{Mod}(\mathbb{D}^1) \cong \mathbb{Z},$$

induced by embedding $\mathbb{D}^b$ into the annulus $\mathbb{D}^1$, capping boundaries other than δ_0 and δ_i with unmarked disks, where the final isomorphism maps the unique positive Dehn twist to 1.

Definition 3.2.1. Given a disk $\mathbb{D}_n^b$ with exterior boundary δ_0, we define the map $D : \mathrm{Mod}(\mathbb{D}_n^b) \to \mathbb{Z}^b$ as $(D_1, \ldots, D_b)$ with each component $D_i : \mathrm{Mod}(\mathbb{D}_n^b) \to \mathbb{Z}$ defined by the composition

$$D_i = \mathit{Cap}_{\delta_0,\delta_i} \circ \mathit{Forget} : \mathrm{Mod}(\mathbb{D}_n^b) \to \mathbb{Z}.$$

Obviously, D maps any arc half-twists to $(0, 0, \ldots, 0)$. Each component D_i maps a positive Dehn twist t_c to 1 when c separates δ_i and the exterior boundary δ_0, or to 0 otherwise. Hence, D_i maps any product of Dehn twists to the total number of Dehn twists separating δ_i from δ_0, counted with sign.

Remark 3.2.2. We note that in the special case without marked points, D is closely related to m_{ij} and m_i as defined in [PVHM10].

The whole reason we introduced this invariant is demonstrated in the next section.

3.3 Replacing marked points with boundaries

This method is best understood through a simple example, so we apply it to the lantern relation in Example 3.4.1.

Example 3.3.1. Projecting and lifting the lantern relation

Projecting the lantern relation (3.4.2) in $\mathrm{Mod}(\mathbb{D}^3)$ seen in left diagram of Figure 3.3 results in the reduced lantern relation (3.4.3) in $\mathrm{Mod}(\mathbb{D}_3)$ shown in the adjacent diagram on the right. In particular, the three interior boundary Dehn twists are no longer in the diagram on the right since they are in the kernel of the capping map $\pi\colon \mathrm{Mod}(\mathbb{D}^3) \to \mathrm{Mod}(\mathbb{D}_3)$. The diagram itself is simply the result of replacing the boundaries with marked points, removing any Dehn twists solely around a single marked point.

Now suppose we attempt to reverse this; namely, we pretend that we do not know the lantern relation in $\mathrm{Mod}(\mathbb{D}^3)$ but do know the reduced lantern relation in $\mathrm{Mod}(\mathbb{D}_3)$, and try to lift the reduced relation to $\mathrm{Mod}(\mathbb{D}^3)$ by replacing the three marked points with boundaries. Each of the Dehn twists individually reverts back to what it was, except for the three interior boundary twists which were in the kernel. The factorizations on the right side matches the original product mapping class, but the one on the left does not, so the two sides are no longer equal.

However, the kernel is generated by the three interior boundary Dehn twists, so there must be some combination of these which we can add back in order to balance the two sides and restore the equality. This is where the invariant helps us, because it tells us exactly what boundary twists we need to make the two sides equal.

Each marked point is enclosed in two Dehn twist curves on the right, but only one on the left, so we need to add to the left a single boundary Dehn twist for each interior boundary, which gives us exactly the relation we started from.

We now formalize this. We have defined the projection π and extended it to relations and factorizations, and now we would like to be able to lift them with respect to π. Since $\mathbb{D}_n^b$ is embedded in $\mathbb{D}_{b+n}$, we can lift any closed curves. We can also lift arcs, but only if neither endpoint is in Q. This means we can lift a Dehn twist t_c for any curve c, but we can only lift an arc half-twist τ_α when α does not have endpoints in Q.

We can extend this to lift words as long as we can lift each twist individually, although we lose uniqueness here since we can always multiply by any element of the kernel to get another lift.

In order to lift a relation in $\mathrm{Mod}(\mathbb{D}_{b+n}, Q)$ to another relation in $\mathrm{Mod}(\mathbb{D}_b^n)$, we need to be able to lift each of the words, but these two lifts also need to have the same product mapping class, and we cannot be sure of this.

We define an *unbalanced relation* in $\mathrm{Mod}(\mathbb{D}_n^b)$ as a pair of words whose product mapping classes are equal modulo a product among $t_{\delta_1}, \cdots, t_{\delta_b}$, and then we define an *unbalanced lift* in $\mathrm{Mod}(\mathbb{D}_n^b)$ of a given relation in $\mathrm{Mod}(\mathbb{D}_{b+n}, Q)$ as an unbalanced relation only requiring that each word lifts from the given relation. We can find an unbalanced lift since we can lift the words individually.

However, given an unbalanced lift, the discrepancy must be in the kernel of π, which is generated by $t_{\delta_1}, \cdots, t_{\delta_b}$. Hence, adjusting them to remove the discrepancy

will not affect the projection, ensuring that the words are still lifts while restoring the balance, giving us a "balanced" lift of the relation.

Knowing that a lift of the relation exists, we simply lift the two sides of the relation individually, creating an unbalanced lift, and then balance it using the invariant D. In a diagram, this means that when a marked point is not the endpoint of any arc half-twists, we can replace it with a boundary, count the number of Dehn twists containing it on either side of the relation, accounting for inverses, and add enough interior boundary twists to balance them.

As a result we can always use $\mathbb{D}_n$, equivalent to the braid group, accounting for boundaries afterwards.

3.4 The lantern relation and associated relations

Here we list some fundamental relations in the planar mapping class groups, which will be used in constructing the main examples of the thesis in Chapter 4. First, we revisit the lantern relation since it is arguably the most important relation in the planar case.

Example 3.4.1. **Lantern Relation**

The *lantern relation* is given by

$$t_{\delta_3} t_{\delta_2} t_{\delta_1} t_{\delta_0} = t_{c_3} t_{c_2} t_{c_1}, \tag{3.4.2}$$

with curves in Figure 3.2 in $\mathbb{D}^3$ on the left, putting the relation in $\mathrm{Mod}(\mathbb{D}^3)$, or in $\mathbb{S}^4$ on the right, putting the relation in the equivalent $\mathrm{Mod}(\mathbb{S}^4)$.

Figure 3.3 shows the equivalent diagram in $\mathrm{Mod}(\mathbb{D}^3)$ on the left, or on the right, the diagram of the reduced relation

$$t_{\delta_0} = t_{c_3} t_{c_2} t_{c_1}, \tag{3.4.3}$$

in Mod($\mathbb{D}_3$), capping three boundaries with singly marked disks.

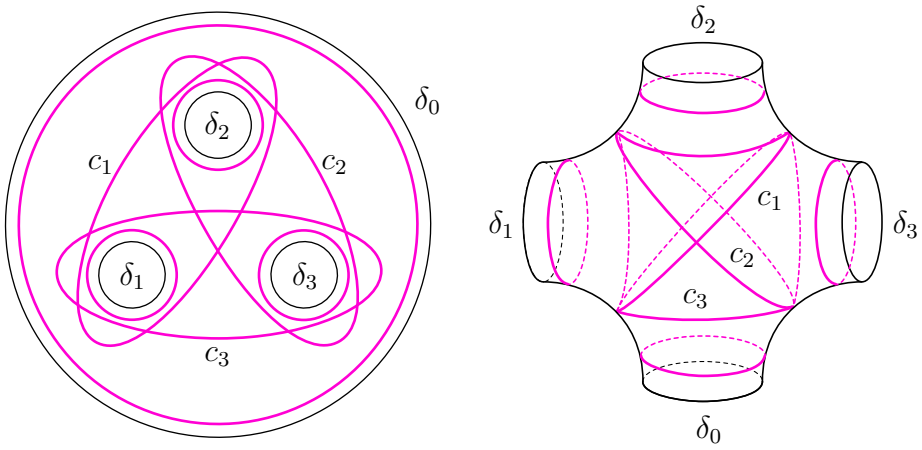

Figure 3.2. The lantern relation curves on $\mathbb{D}^3$ (left) and on $\mathbb{S}^4$ (right).

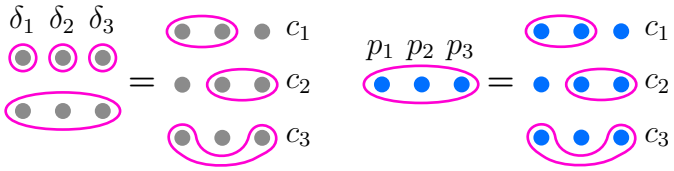

Figure 3.3. Left: The lantern relation in Mod($\mathbb{D}^3$) with an exterior boundary and three interior boundaries. Right: The reduced lantern relation in Mod($\mathbb{D}_3$) with an exterior boundary and three marked points, which results from capping the three interior boundaries with once marked disks.

Example 3.4.4. **Half Lantern Relation**

We introduce the relation

$$t_{\delta_1}^2 t_{\delta_0} = \tau_\beta \tau_\alpha t_c^2 \tag{3.4.5}$$

defined in Mod($\mathbb{D}_2^1$) as shown on the left of Figure 3.5 with the corresponding reduced relation

$$t_{\delta_0} = \tau_\beta \tau_\alpha t_c^2 \tag{3.4.6}$$

shown on the right of the same figure. We refer to the first as the *half lantern relation*, since it lifts via the Birman-Hilden double cover to the lantern relation in Figure 3.2

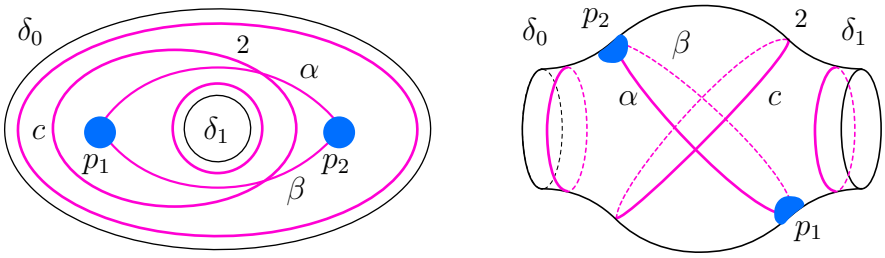

Figure 3.4. The half lantern relation curves and arcs in $\mathbb{D}_2^1$ (left) and on $\mathbb{S}_2^2$ (right).

as shown below in Figure 3.6. This relation has been helpful in many other derivations similar to the way it is used in the third step of Figure 4.7, essentially to get rid of inverse twists in exchange for arc half-twists, provided there is another Dehn twist with the same configuration.

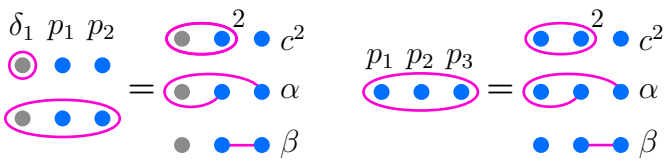

Figure 3.5. Left: The half lantern relation in $\mathrm{Mod}(\mathbb{D}_2^1)$. Right: The reduced half lantern relation in $\mathrm{Mod}(\mathbb{D}_3)$.

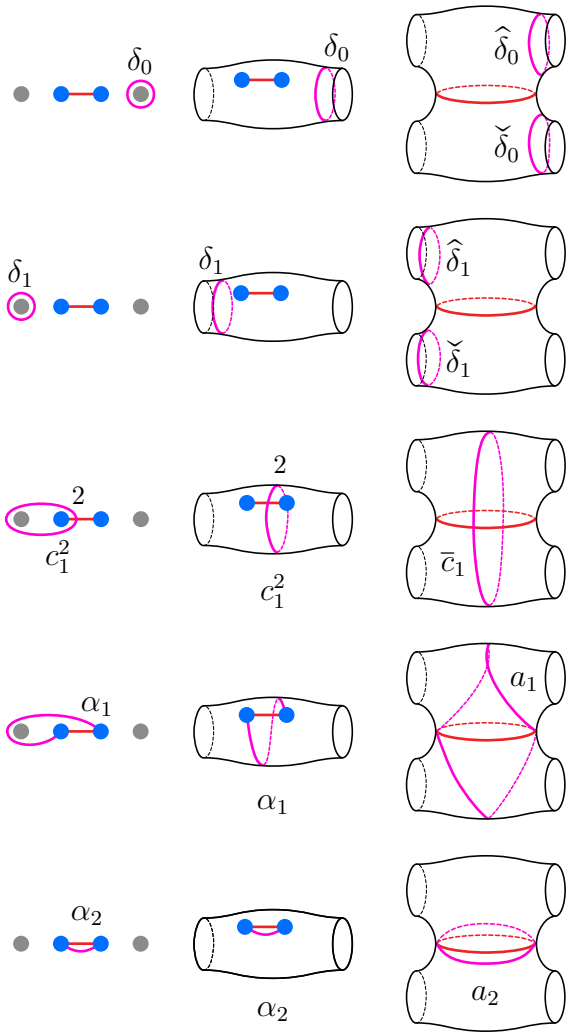

Figure 3.6. Lifting the half lantern relation curves in $\mathbb{S}_2^2$ to the lantern relation curves in $\mathbb{S}^4$.

Example 3.4.7. **Daisy Relation**

The daisy relation with $n \geq 3$ interior boundaries is given by

$$t_{\delta_n}^{n-2} t_{\delta_{n-1}} \cdots t_{\delta_0} = t_{c_n} t_{c_{n-1}} \cdots t_{c_1} \tag{3.4.8}$$

in $\text{Mod}(\mathbb{D}^n) = \text{Mod}(\mathbb{S}^{n+1})$ where the curves and boundaries are shown in Figure 3.7 in two equivalent forms. On the left of the figure, the curves are in $\mathbb{D}^n$ as introduced in [PVHM10]. On the right, the curves are in $\mathbb{S}^{n+1}$ as introduced in [EMVHM11], referred to as the daisy relation because of this shape. The daisy relation is a generalization of the lantern relation as it contains the lantern relation as the special case with $n = 3$.

We represent the daisy relation in the diagram in $\mathbb{D}^n$ on the left of Figure 3.8. If we cap all the interior boundaries with once marked disks we obtain a reduced form of the daisy relation

$$t_{\delta_0} = t_{c_n} t_{c_{n-1}} \cdots t_{c_1} \tag{3.4.9}$$

in $\text{Mod}(\mathbb{D}_n)$ as in the right of Figure 3.8.

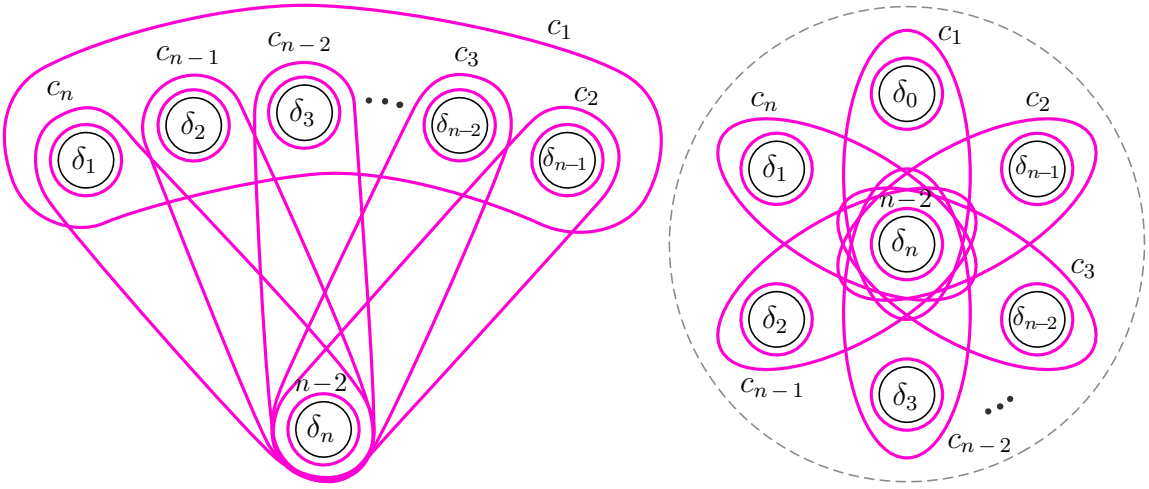

Figure 3.7. The daisy relation curves in $\mathbb{D}^n$ as in [PVHM10] (left) and in $\mathbb{S}^{n+1}$ as in [EMVHM11](right).

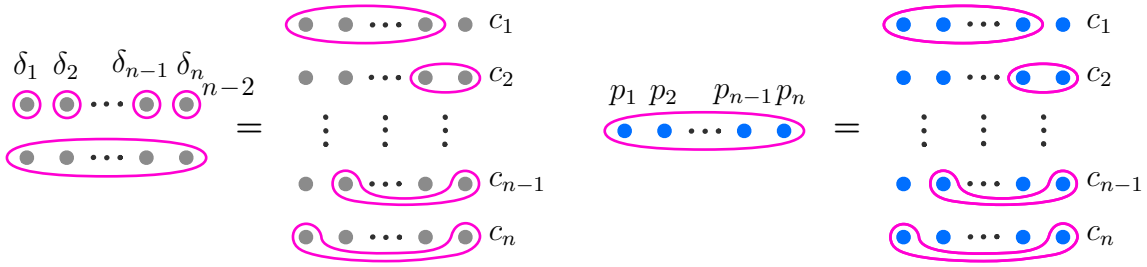

Figure 3.8. Left: The usual daisy relation in $\mathrm{Mod}(\mathbb{D}^n)$ with an exterior boundary and n interior boundaries, which factorizes $t_{\delta_n}^{n-2} t_{\delta_{n-1}} \cdots t_{\delta_0}$. Right: The reduced daisy relation in $\mathrm{Mod}(\mathbb{D}_n)$ with an exterior boundary and n marked points, which now factorizes only t_{δ_0} as the interior boundary twists reduced to the identity.

CHAPTER 4

GENERALIZING THE BAYKUR-KORKMAZ POSITIVE FACTORIZATION

In [BK17], Baykur and Korkmaz derive an explicit positive factorization that produces the smallest genus-2 Lefschetz fibration with 7 vanishing cycles, which has 4 nonseparating and 3 separating. Baykur and Hamada have found a lift of this positive factorization that locates three exceptional sections of the fibration [BH, Bay22]. Moreover, Baykur, Hamada and Korkmaz have generalized this to a genus $g \geq 2$ hyperelliptic Lefschetz fibration with $5g-3$ vanishing cycles, $4g-4$ nonseparating and $g+1$ separating, together with $g+1$ exceptional sections (private communication). Using our methods, we obtain similar positive factorizations that produce a genus g hyperelliptic Lefschetz fibration with $g+1$ exceptional sections for each $g \geq 2$, to which we refer collectively as X_{BK}.

In what follows we first present the resultant relations in the planar mapping class groups without derivation and give their lifts in higher genera mapping class groups, which are the positive factorizations for our Lefschetz fibrations X_{BK}. The constructions of those planar relations will be given afterwards.

4.1 The genus 2 case

We start with the genus 2 case. The relation

$$t_{\delta_2}^2 t_{\delta_1}^2 t_{\delta_0}^2 = \tau_{\alpha_4}\tau_{\alpha_3}\tau_{\alpha_2} t_e^2 \tau_{\alpha_1} t_d^2 t_c^2 \tag{4.1.1}$$

is defined in $\mathrm{Mod}(\mathbb{S}_3^3)$ with the curves and arcs in Figure 4.1. The derivation will be given in Section 4.3 below.

Consider the Birman-Hilden double cover $\Sigma_2^3 \to \mathbb{S}_3^3$ as specified in Figure 4.2. We can lift the relation, as all factors are liftable, to obtain the new relation

$$t_{\bar{\delta}_2} t_{\bar{\delta}_1} t_{\bar{\delta}_0} = t_{a_4} t_{a_3} t_{a_2} t_{\bar{e}} t_{a_1} t_{\bar{d}} t_{\bar{c}}, \tag{4.1.2}$$

in $\mathrm{Mod}(\Sigma_2^3)$ as shown in Figure 4.2. This is a positive factorization of the boundary multitwist, giving a genus 2 Lefschetz fibration X_{BK} with 7 vanishing cycles, 4 non separating and 3 separating, together with 3 exceptional sections.

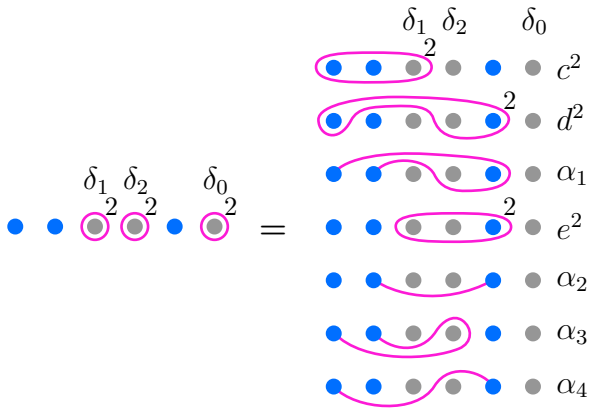

Figure 4.1. The factorization of $t_{\delta_2}^2 t_{\delta_1}^2 t_{\delta_0}^2$ in $\mathrm{Mod}(\mathbb{S}_3^3)$.

4.2 Arbitrary genus $g \geq 2$ case

Moving to the general genus $g \geq 2$ case, we consider the planar relation

$$t_{\delta_g}^2 t_{\delta_{g-1}}^2 \cdots t_{\delta_0}^2 = \tau_{\alpha_{4g-4}} \tau_{\alpha_{4g-5}} \cdots \tau_{\alpha_g} t_e^2 \tau_{\alpha_{g-1}} t_{d_{g-1}}^2 \tau_{\alpha_{g-2}} t_{d_{g-2}}^2 \cdots \tau_{\alpha_1} t_{d_1}^2 t_c^2, \tag{4.2.1}$$

in $\mathrm{Mod}(\mathbb{S}_{g+1}^{g+1})$ shown in Figure 4.3. The derivation will be given in Section 4.4 below.

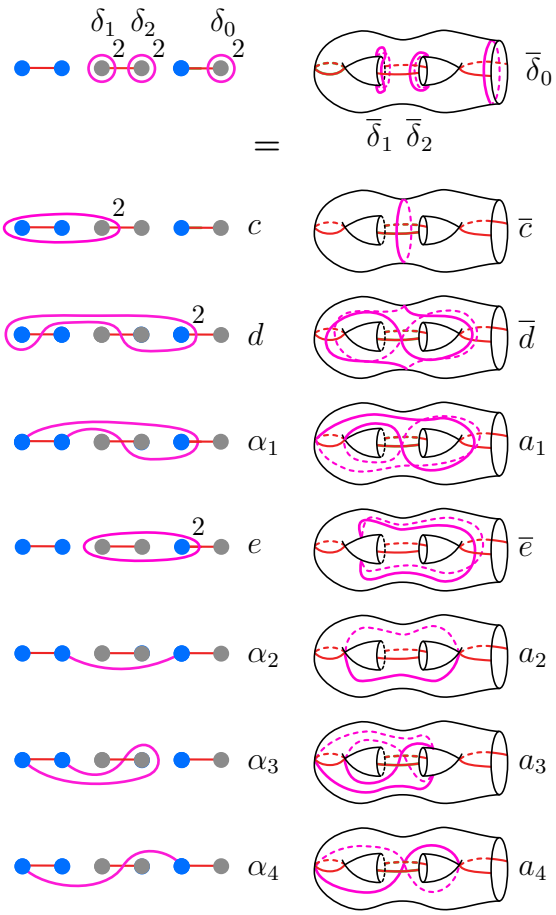

Figure 4.2. Lifting the planar relation (4.1.1) in Figure 4.1 from $\mathrm{Mod}(\mathbb{S}_3^3)$ to obtain a positive factorization of the boundary multitwist $t_{\overline{\delta}_2} t_{\overline{\delta}_1} t_{\overline{\delta}_0}$ in $\mathrm{Mod}(\Sigma_2^3)$. The latter defines the genus 2 Lefschetz fibration X_{BK} with three explicit exceptional sections.

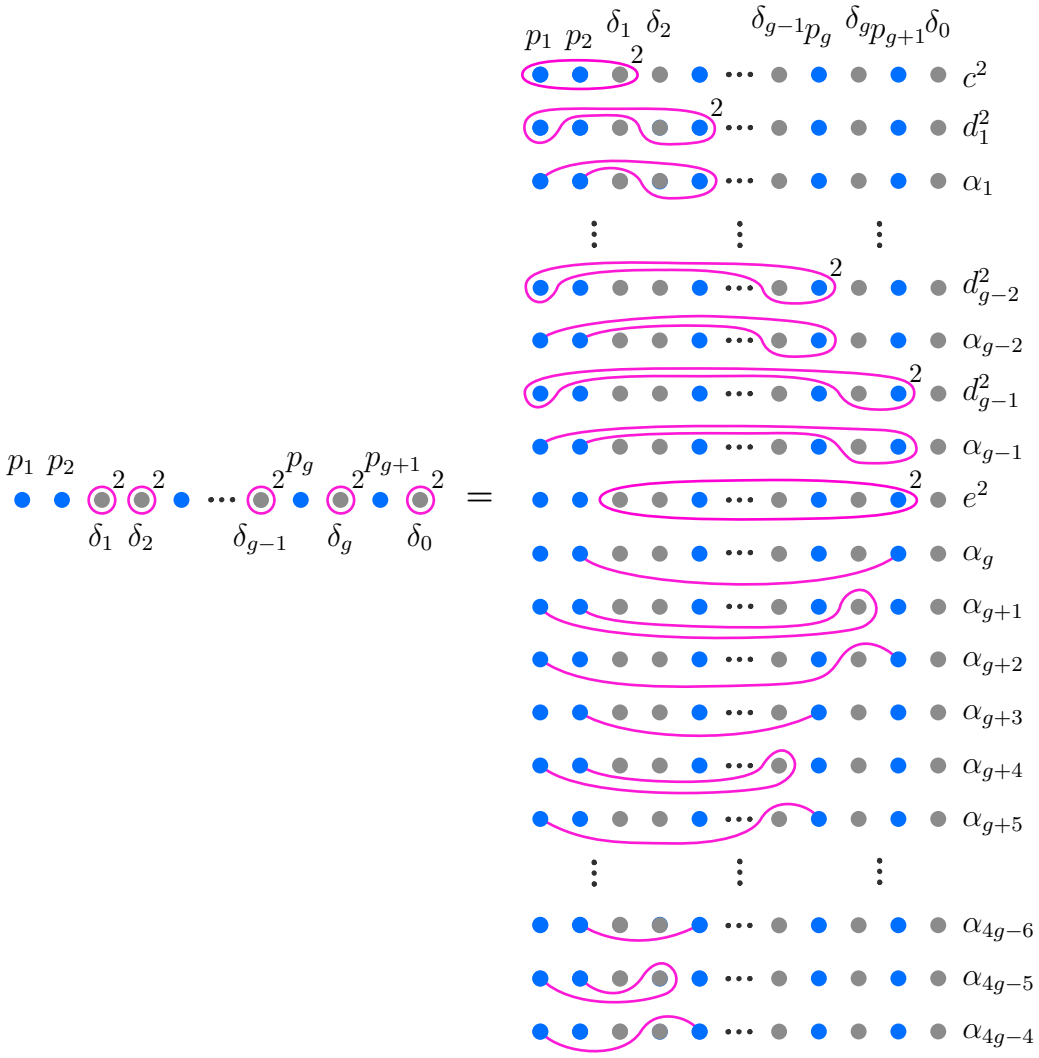

Figure 4.3. The factorization of $t_{\delta_g}^2 t_{\delta_{g-1}}^2 \cdots t_{\delta_0}^2$ in $\mathrm{Mod}(\mathbb{S}_{g+1}^{g+1})$.

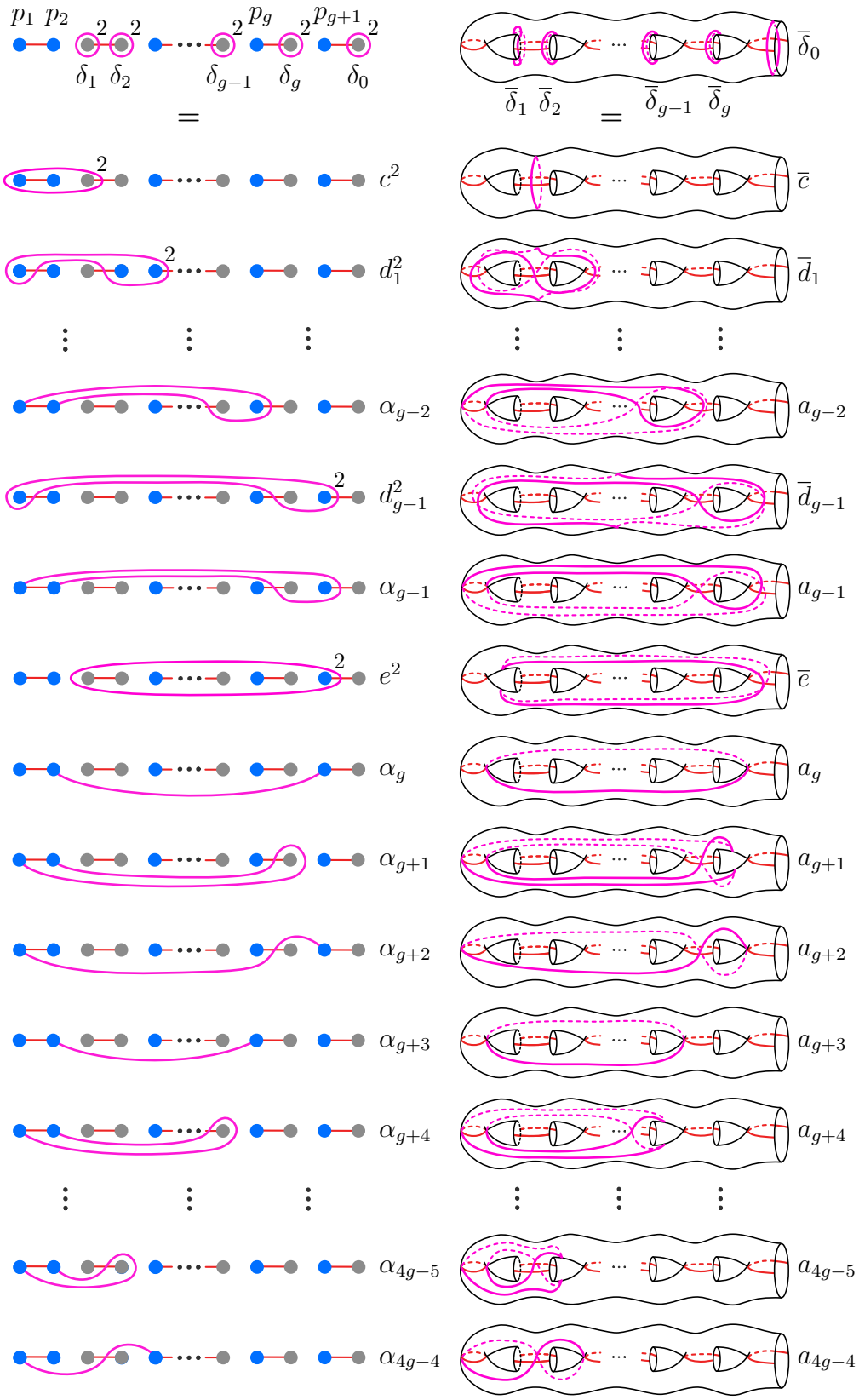

Figure 4.4. Lifting the planar relation (4.2.1) in Figure 4.3 from $\mathrm{Mod}(\mathbb{S}_{g+1}^{g+1})$ to obtain the positive factorization of the boundary multitwist in $\mathrm{Mod}(\Sigma_g^{g+1})$. The latter defines the genus g Lefschetz fibration X_{BK} with $g+1$ explicit exceptional sections.

We can lift this with respect to the Birman-Hilden double cover $\Sigma_g^{g+1} \to \mathbb{S}_{g+1}^{g+1}$ to obtain the relation

$$t_{\bar{\delta}_g} t_{\bar{\delta}_{g-1}} \cdots t_{\bar{\delta}_0} = t_{a_{4g-4}} t_{a_{4g-5}} \cdots t_{a_g} t_{\bar{e}} t_{a_{g-1}} t_{\bar{d}_{g-1}} t_{a_{g-2}} t_{\bar{d}_{g-2}} \cdots t_{a_1} t_{\bar{d}_1} t_{\bar{c}}, \tag{4.2.2}$$

in $\mathrm{Mod}(\Sigma_g^{g+1})$ as demonstrated in Figure 4.4. This gives a genus g Lefschetz fibration with $6g-5$ vanishing cycles, $4g-4$ non separating and $g+1$ separating, together with $g+1$ exceptional sections. Moreover, this fibration is hyperelliptic as the monodromy factorization is obtained via the Birman-Hilden theory without symmetric pairs of Dehn twists.

4.3 Derivation: The base case with $g = 2$

We now construct the relation (4.2.1) by induction on g. As the base case we first derive the relation with $g = 2$, which is singled out as the relation (4.1.1) and in Figure 4.1.

Proof. Consider the daisy relation in $\mathrm{Mod}(\mathbb{D}^4)$ with an exterior boundary and 4 interior boundaries, as displayed on the right of Figure 3.8 (with $n = 4$). We cap the first three interior boundaries from left with once-marked disks, whereas we cap the rightmost boundary with a twice-marked disk. This results in a factorization of the exterior boundary twist t_{δ_0} in $\mathrm{Mod}(\mathbb{D}_5)$ as show in the first diagram of Figure 4.5. Note that the squared negative Dehn twist comes from the rightmost interior boundary twist of the original daisy relation.

The second and third diagrams in Figure 4.5 also show factorizations of t_{δ_0}. Both of them are obtained from the first diagram, by a cyclic permutation and by rearranging the marked points, respectively, as illustrated in Figures 4.5 and 4.6.

Next we combine the second and third factorizations of t_{δ_0} in Figure 4.5 to obtain a factorization of $t_{\delta_0}^2$ as shown in the first diagram of Figure 4.7. With a cyclic

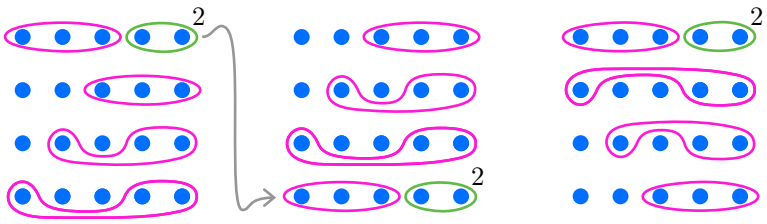

Figure 4.5. Three factorizations of the exterior boundary twist t_{δ_0} in $\mathrm{Mod}(\mathbb{D}_5)$. The first is a reduced daisy relation. The second follows immediately with cyclic permutation. The third is obtained from the first by rearranging the marked points as shown in Figure 4.6. Recall that green curves with index 2 represent squared negative Dehn twists.

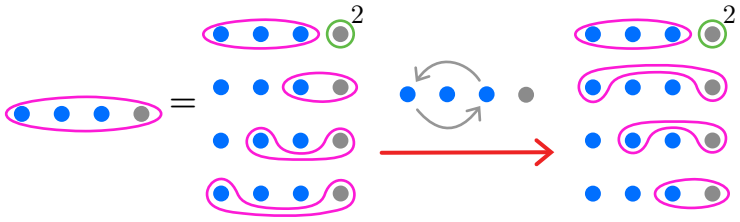

Figure 4.6. Rearranging the first and third marked points by dragging them around the second marked point.

permutation and commutativity relations, we cluster some of the Dehn twists to form squares as in the third diagram of Figure 4.7. Now in that diagram, there are two pairs located at the bottom: each consists of a positive Dehn twist and a squared negative Dehn twist. By utilizing appropriately configured half lantern relations, we can substitute these pairs with pairs of half-twists, which results in the fourth diagram of Figure 4.7. This gets rid of all the negative Dehn twists.

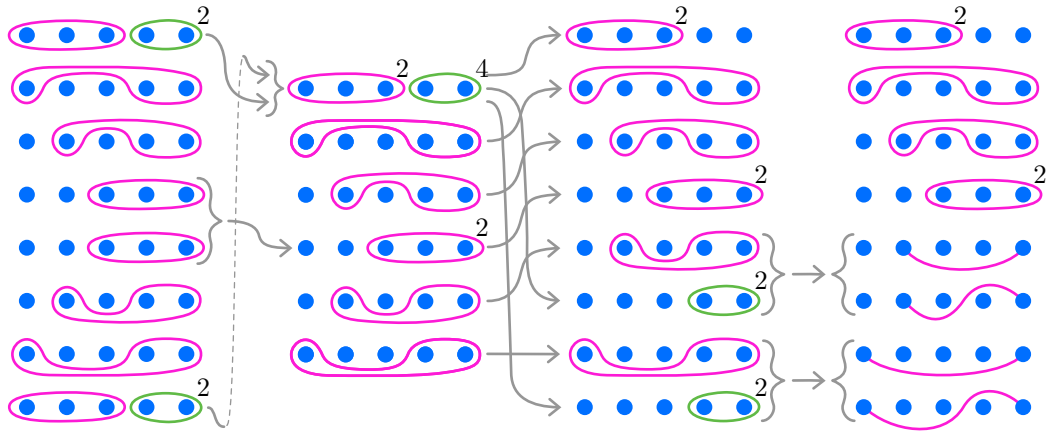

Figure 4.7. Factorizations of $t_{\delta_0}^2$ in $\mathrm{Mod}(\mathbb{D}_5)$. The first is the concatenation of the third and second diagrams in Figure 4.5. Through cyclic permutation and commutativity relations, we reach the third diagram. The fourth diagram is then obtained by substitution using the half lantern relation twice.

Notice that there are two unliftable Dehn twists of odd parity, which are located in the second and third rows of the first diagram of Figure 4.8. The next step is to modify the pair into a liftable squared Dehn twist. This is achieved by a series of Hurwitz moves as indicated in Figure 4.8.

Finally, we lift the last factorization in $\mathrm{Mod}(\mathbb{D}_5)$ to $\mathrm{Mod}(\mathbb{D}_3^2)$ and then rearrange the diagram to be presented in $\mathrm{Mod}(\mathbb{S}_3^3)$ as shown in Figure 4.9. First, replacing the third and fourth marked points in $\mathbb{D}_5$ with boundaries, we embed $\mathbb{D}_3^2$ into $\mathbb{D}_5$. The last factorization of $t_{\delta_0}^2$ in $\mathrm{Mod}(\mathbb{D}_5)$ (Figure 4.8) can be lifted to a factorization in $\mathrm{Mod}(\mathbb{D}_3^2)$ (the left in Figure 4.9) as all the half-twists avoid the replaced marked

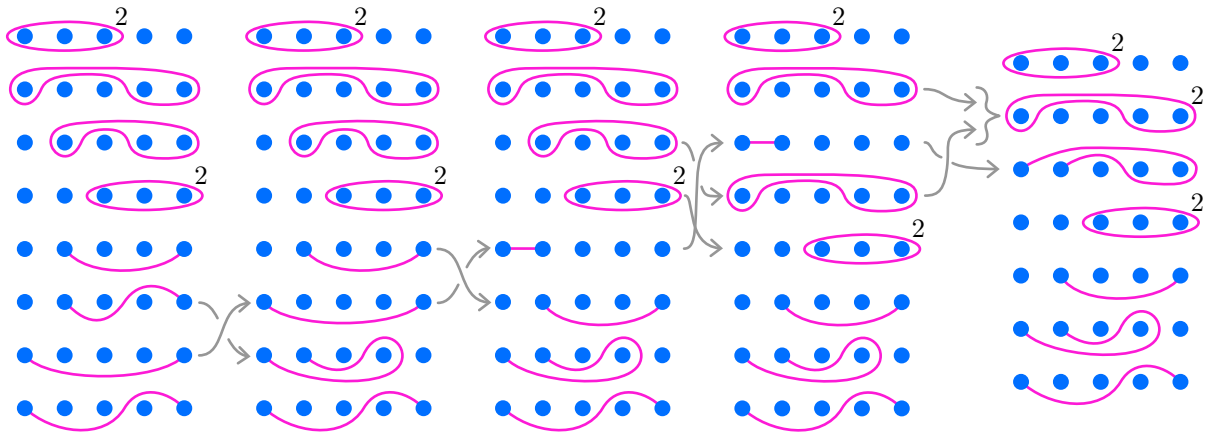

Figure 4.8. Hurwitz moves among factorizations of $t^2_{\delta_0}$ in $\mathrm{Mod}(\mathbb{D}_5)$. The fifth diagram now contains only liftable factors.

points. Notice that the extra boundary twists have been added to balance the Dehn twist invariant (See Section 3.3). On the right of Figure 4.9 we move the factorization to a spherical diagram putting the exterior boundary on the right (and isotoping the exterior boundary twist around the sphere with it). This is the desired factorization of $t^2_{\delta_2} t^2_{\delta_1} t^2_{\delta_0}$ in $\mathrm{Mod}(\mathbb{S}^3_3)$. □

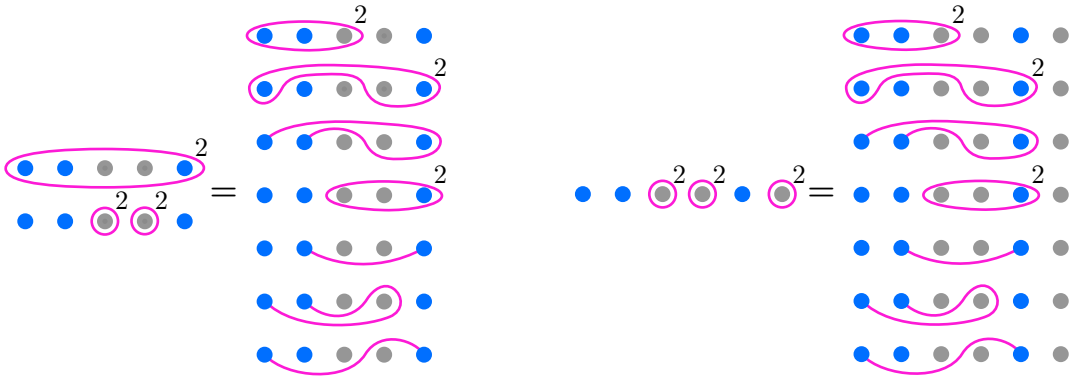

Figure 4.9. The factorization of $t^2_{\delta_2} t^2_{\delta_1} t^2_{\delta_0}$ in $\mathrm{Mod}(\mathbb{D}^2_3) = \mathrm{Mod}(\mathbb{S}^3_3)$ seen on the disk $\mathbb{D}^2_3$ (left) and on the sphere $\mathbb{S}^3_3$ (right). From the last relation in $\mathrm{Mod}(\mathbb{D}_5)$ in Figure 4.8, replacing two marked points with boundaries gives the relation on the left.

4.4 Derivation: The inductive step for arbitrary $g \geq 2$

To prove the general relation (4.2.1) in $\mathrm{Mod}(\mathbb{S}^{g+1}_{g+1})$ in Figure 4.3, we first observe this is equivalent to the relation in $\mathrm{Mod}(\mathbb{D}^{g}_{g+1})$ described in Figure 4.10 after a cyclic permutation, although the first is drawn on a sphere while the second is drawn on a disk. Hence it suffices to prove the second relation, which will be more convenient for the inductive step.

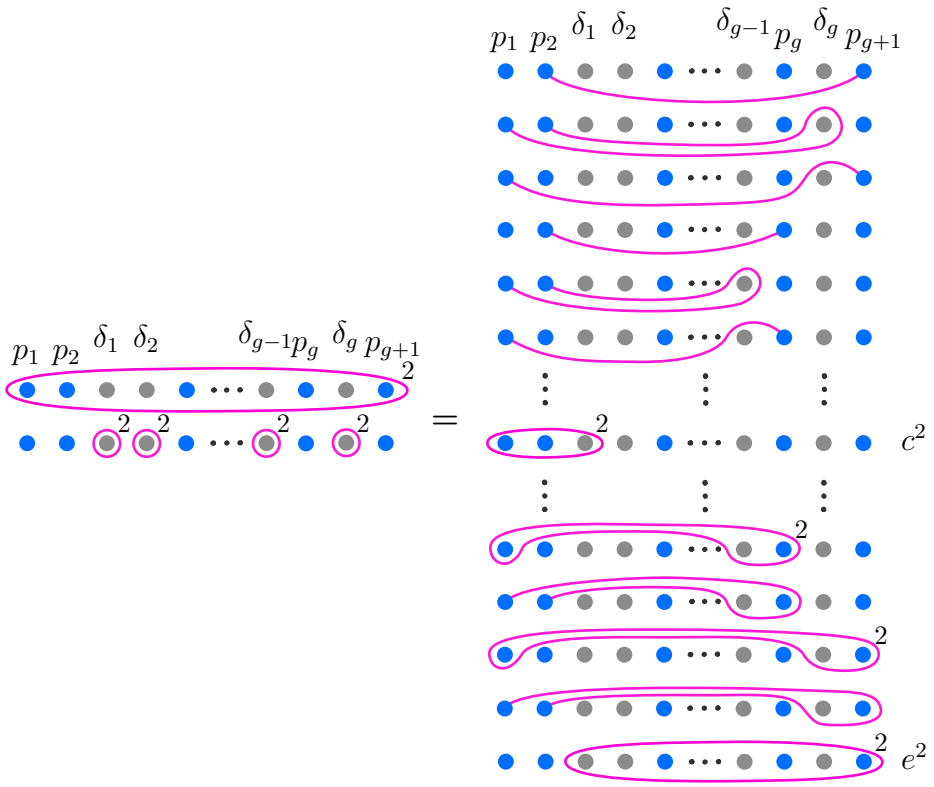

Figure 4.10. The factorization of $t^2_{\delta_g} t^2_{\delta_{g-1}} \cdots t^2_{\delta_0}$ in $\mathrm{Mod}(\mathbb{D}^{g}_{g+1})$.

Proof. As we use the induction, we will derive the relation in $\mathrm{Mod}(\mathbb{D}^{g}_{g+1})$ in Figure 4.10 assuming the same relation holds when g is replaced by $g-1$. Since we can recover the information on the boundary twists at the end using the Dehn twist invariant, we will work on the simpler $\mathrm{Mod}(\mathbb{D}_{2g+1})$ with all the interior boundaries of $\mathbb{D}^{g}_{g+1}$ being replaced with marked points.

First, we take the subsurface of $\mathbb{D}_{2g+1}$ bounded by the exterior boundary, the curve enclosing the middle $2g-3$ marked points, and the curve around the second marked point from right. This subsurface is homeomorphic to $\mathbb{D}^2_3$, hence we can use the already established relation in Figure 4.10 with $g=2$, which is displayed in Figure 4.11. Note that the boundary twist that encloses the single marked point reduced to 1 and hence does not appear in the diagram.

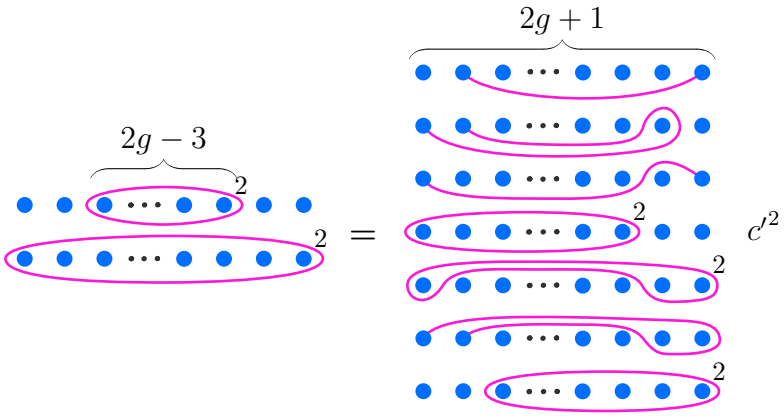

Figure 4.11. The relation in $\mathrm{Mod}(\mathbb{D}_{2g+1})$ induced from the $g=2$ relation.

The curve labeled c' bounds a disk homeomorphic to $\mathbb{D}_{2g-2}$. This is where we substitute the $g-1$ relation, after converting its interior boundaries to marked points. The resulting relation is shown in Figure 4.12.

On the right diagram in Figure 4.12, we can commute the Dehn twist labeled e' to the bottom and then cancel it with the same Dehn twist on the left diagram. The result of this is the desired relation in Figure 4.10 except that the interior boundaries are replaced by marked points. We recover the interior boundaries by usign the Dehn twist invariant: We convert the third marked point, along with every even marked point other than the second, to a boundary. To balance the Dehn twist invariant, we need to add squared interior boundary twists on the left. This finally proves the relation in Figure 4.10. □

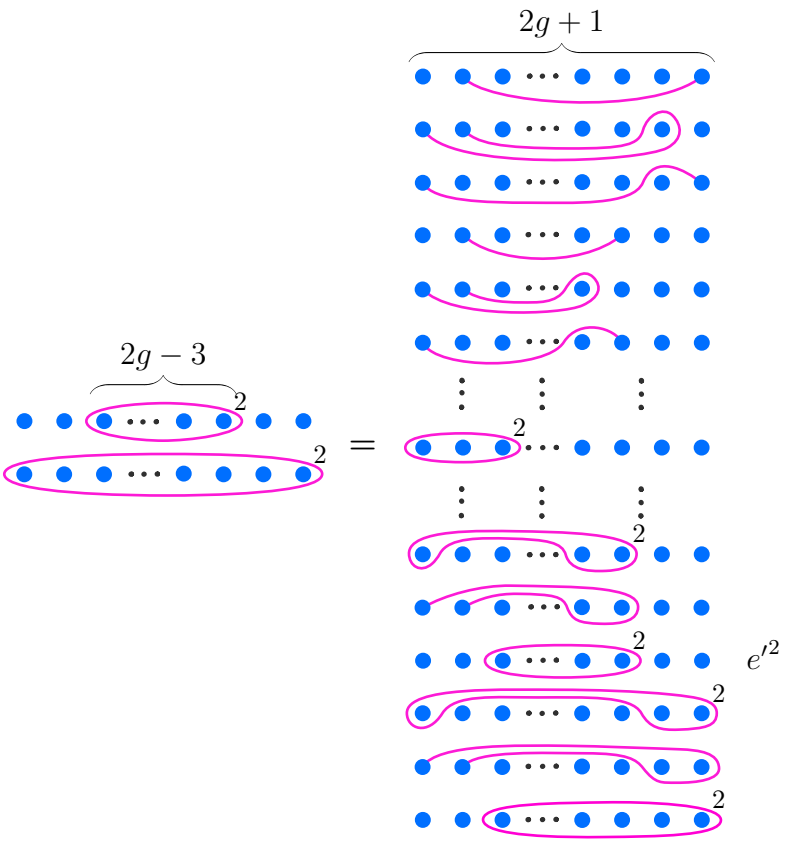

Figure 4.12. The relation in $\mathrm{Mod}(\mathbb{D}_{2g+1})$ obtained by combining the $g = 2$ and $g-1$ relations.

CHAPTER 5

ALGEBRAIC TOPOLOGY OF SYMMETRIC LEFSCHETZ FIBRATIONS

A Lefschetz fibration is *hyperelliptic* when each of the Dehn twists in the monodromy factorization commutes with a fixed hyperelliptic involution. This is equivalent to when all the monodromy curves (up to isotopy) are fixed by the same hyperelliptic involution; we call them *symmetric* in this case. This excludes vanishing cycles which form symmetric *pairs*, despite the corresponding pair of Dehn twists together forming a hyperelliptic mapping class, since the Dehn twists are not individually hyperelliptic. This leads us to define the slightly larger class of *symmetric* Lefschetz fibrations. In keeping with the spirit of this thesis, we determine how to calculate the signatures of symmetric Lefschetz fibrations (as a slight extension of Endo's signature formula) directly using the arcs and curves of the planar surface.

5.1 Signatures of symmetric Lefschetz fibrations

We recall Endo's result [End00] giving a formula for the signature of hyperelliptic Lefschetz fibrations as a sum of local contributions from each vanishing cycle depending only on their topological type and the genus of the fibration. We say a vanishing cycle c has topological type I if it is symmetric (with respect to a fixed hyperelliptic involution on the surface) and nonseparating. On a genus g surface, for each h with $1 \leq h \leq \lfloor g/2 \rfloor$, we say a vanishing cycle has topological type II_h if it is symmetric and separates the surface into components having genus h and $g-h$.

Lemma 5.1.1 (Endo's signature formula for hyperelliptic Lefschetz fibrations)**.** *Given a genus g hyperelliptic Lefschetz fibration on a 4-manifold X with monodromy factorization*

$$t_{c_\ell} \cdots t_{c_2} t_{c_1} = 1$$

in $\mathrm{Mod}(\Sigma_g)$*, let* n_{I} *be the number of vanishing cycles of type* I*, and for each* h *with* $1 \leq h \leq \lfloor g/2 \rfloor$*, let* n_h *be the number of vanishing cycles of type* II_h*. Then each vanishing cycle's signature contribution is given by the corresponding formula:*

$$\sigma_g(\mathrm{I}) = \frac{-(g+1)}{2g+1}$$

for type I *curves, and*

$$\sigma_g(\mathrm{II}_h) = \frac{4h(g-h)}{2g+1} - 1$$

for type II_h *curves, so that given the genus* g*, the signature is given by*

$$\sigma(X) = n_{\mathrm{I}}\sigma_g(\mathrm{I}) + \Sigma_{h=1}^{\lfloor g/2 \rfloor} \left(n_h \sigma_g(\mathrm{II}_h) \right).$$

Although all Lefschetz fibrations coming from a double cover of a planar surface will be symmetric by definition, many of them are not hyperelliptic because of the symmetric pairs of curves that are not individually hyperelliptic. In this case, we can still calculate the signature without completely losing the above simplicity by using substitutions to exchange problematic vanishing cycles with equivalent completely hyperelliptic products, calculating the changes using the signature of relations in [EN05].[1]

The result fits nicely with the original formula, suggesting an additional topological type. Given a genus g surface, for each h with $1 \leq h \leq \lfloor (g-1)/2 \rfloor$, we propose

[1] I would like to thank my advisor İnanç Baykur for suggesting this argument.

calling a symmetric pair of vanishing cycles c_1 and c_2 of topological type III_h when c_1 and c_2 separating the surface into components having genus h and $g-h-1$, while c_1 and c_2 are individually non-separating and non-symmetric.

Corollary 5.1.2 (Signatures of symmetric Lefschetz fibrations)**.** *Given a genus g symmetric Lefschetz fibration on a 4-manifold X with monodromy factorization*

$$t_{c_\ell} \cdots t_{c_2} t_{c_1} = 1$$

in $\text{Mod}(\Sigma_g)$*, let* n_{I}*,* n_h*,* $\sigma_g(\text{I})$*, and* $\sigma_g(\text{II}_h)$ *be defined as in Lemma 5.1.1, and for each* h *with* $1 \leq h \leq \lfloor (g-1)/2 \rfloor$*, let* m_h *be the number of vanishing cycles of type* III_h*. Then each type* III_h *vanishing cycle pair's additional signature contribution is given by*

$$\sigma_g(\text{III}_h) = \frac{2(h+1)(g-h)}{2g+1} - 2$$

so that given the genus g, the signature is given by

$$\sigma(X) = n_{\text{I}}\sigma_g(\text{I}) + \Sigma_{h=1}^{\lfloor g/2 \rfloor} \left(n_h \sigma_g(\text{II}_h)\right) + \Sigma_{h=1}^{\lfloor (g-1)/2 \rfloor} \left(m_h \sigma_g(\text{III}_h)\right).$$

Proof. We just have to account for the third equation. With our setup, the symmetric pairs correspond to Dehn twists lifted from even parity Dehn twists, each of which separate the planar surface into components with $2h+2$ and $2(g-h)$ marked points for some $h \leq \lfloor (g-1)/2 \rfloor$. We can make a substitution to replace them with $(2h+1)(2h+2)$ arc half-twists, with the lifted substitution corresponding to a $2h+1$-chain relation, replacing the separating pair with $(2h+1)(2h+2)$ symmetric nonseparating curves. This results in an exchange of signature contributions replacing $I(c_{2h+1}) = -2h(h+$

2) with $(2h+1)(2h+2)\sigma_g(\mathrm{I})$, so the difference determines the contribution of the symmetric pair:

$$\begin{aligned}
\sigma_g(\mathrm{III}_h) = \Delta\sigma &= (2h+1)(2h+2)\sigma_g(\mathrm{I}) - I(c_{2h+1}) \\
&= 2h(h+2) - \frac{(2h+1)(2h+2)(g+1)}{2g+1} \\
&= \frac{1}{2g+1}\left((2h^2+4h)(2g+1) - (4h^2+6h+2)(g+1)\right) \\
&= \frac{1}{2g+1}\left(4h^2g + 2h^2 + 8gh + 4h - 4h^2g - 4h^2 - 6hg - 6h - 2g - 2\right) \\
&= \frac{2hg - 2h^2 - 2h - 2g - 2}{2g+1} \\
&= \frac{2((h+1)(g-h) + (2g+1))}{2g+1} \\
&= \frac{2(h+1)(g-h)}{2g+1} - 2.
\end{aligned} \tag{5.1.3}$$

□

Corollary 5.1.4. *Given a 4-manifold X having a symmetric Lefschetz fibration with monodromy factorization lifted through a double cover from a planar factorization, we can calculate the signature directly from the planar factorization using the same formulas as Corollary 5.1.2 by letting n_{I} be the number of arc half-twists, letting n_h be the number of squared odd parity Dehn twists, and letting m_h be the number of even parity Dehn twists.*

Proof. This follows directly from Corollary 5.1.2 by taking into account how the different types of twists are lifted, since arc half-twists lift to Dehn twists around type I curves, squared odd parity Dehn twists lift to type II curves, and even parity Dehn twists lift to pairs of type III curves. □

5.2 First homology of Lefschetz fibrations

Given a 4-manifold X with a genus g Lefschetz fibration $f\colon X \to S^2$, we can calculate the first homology by considering the induced handle decomposition corresponding to the monodromy factorization

$$t_{c_\ell} \cdots t_{c_2} t_{c_1} = 1$$

in $\mathrm{Mod}(\Sigma_g)$. Assuming (X, f) has a section,

$$H_1(X;\mathbb{Z}) \cong H_1(\Sigma_g;\mathbb{Z}) \,/\, N$$

where N is the subgroup of $H_1(\Sigma_g;\mathbb{Z})$ normally generated by the vanishing cycles $c_1, \ldots, c_\ell$. (A priori there may be one more relation if (X, f) does not have a section. However, all the examples we consider in this thesis are easily seen to have sections.)

While we can make different choices of generators for $H_1(\Sigma_g;\mathbb{Z})$ to make our calculations more efficient, we would typically start with the standard symplectic basis seen in Figure 5.1 given by g pairs of oriented curves $\{a_1, b_1, \ldots, a_g, b_g\}$ representing homology classes, so that $a_i \cdot b_j = \delta_{ij}$ and $a_i \cdot a_j = b_i \cdot b_j = 0$ for $1 \leq i, j \leq g$ where $\delta_{ij} = 1$ when $i = j$ and 0 otherwise. In this basis, the homology class of each vanishing cycle c_i with $1 \leq i \leq \ell$ can then be expressed as

$$\sum_{j=1}^{g} ((c_i \cdot b_j)a_j - (c_i \cdot a_j)b_j\,). \tag{5.2.1}$$

Remark 5.2.2. As with the signature, it also possible to calculate the homology classes of each vanishing cycle c_i in $\widetilde{S}$ directly in the planar surface S by considering how intersections with α_i or $\underline{b}_i$ in S (see the bottom of Figure 5.1) will correspond to intersections of c_i with a_i or b_i in $\widetilde{S}$, carefully keeping track of interactions with the branch cuts and marked points to account for the differing contributions on the upper and lower sheets.

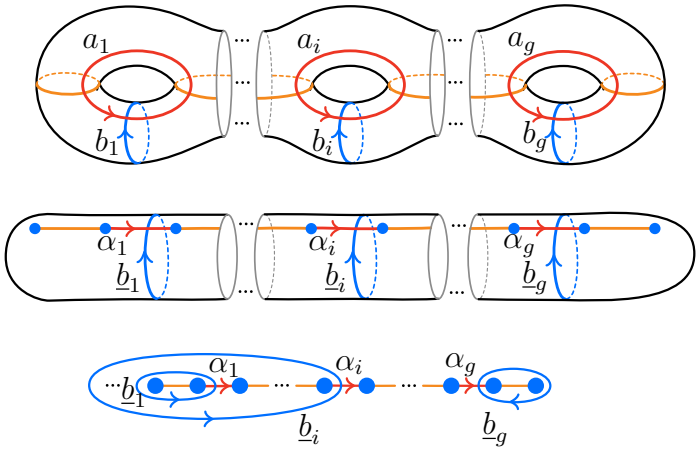

Figure 5.1. Curves in $\widetilde{S} = \Sigma_g$ representing homology classes for the standard symplectic basis of $H_1(\widetilde{S}; \mathbb{Z})$ (top) are projected to curves or arcs in $S = \mathbb{S}_{2g+2}$ in a spherical diagram (middle) or a planar diagram (bottom).

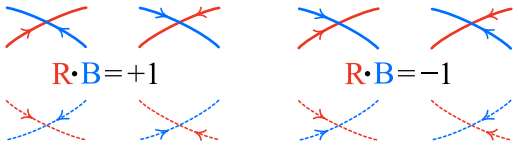

Figure 5.2. Right-handed intersections on the left, and left-handed intersections on the right.

CHAPTER 6

SHARPNESS THEOREM

6.1 Known inequalities on the number of vanishing cycles

Given a genus g Lefschetz fibration $f\colon X \to S^2$ with ℓ vanishing cycles, let n and s be the number of nonseparating and separating vanishing cycles of the fibration (X, f). Let e be the Euler characteristic of X, b_i be its $i-$th Betti number. Let b^+ and b^- be the dimensions of the positive and negative eigenspaces associated to the intersection form of X, and let σ be the signature.

The following inequalities are well known to the experts; see e.g. [BK17] for the latter. We include proofs for completeness.

Theorem 6.1.1. *The following inequalities hold for any genus g Lefschetz fibration (X, f) with the invariants listed above:*

$$n \geq 4g - 2b_1(X) + b^+(X) - 1, \tag{6.1.2}$$

$$s \leq b^-(X) - 1. \tag{6.1.3}$$

Proof. Cadavid [Cad98] showed that

$$\sigma \leq n - s - 2(2g - b_1). \tag{6.1.4}$$

The handle decomposition induced by the Lefschetz fibration on X yields the equality:

$$\begin{aligned} e &= e(\Sigma_g)\, e(S^2) + \ell \\ &= (2-2g)2 + \ell \\ &= 4 - 4g + n + s. \end{aligned} \tag{6.1.5}$$

We can also express the Euler characteristic of X in terms of its Betti numbers. Since X is connected, $b_0 = 1$, and since it is closed and orientable, we know from Poincaré duality and the universal coefficients theorem that $b_4 = b_0$ and $b_3 = b_1$. By definition, $b_2 = b^+ + b^-$ and $\sigma = b^+ - b^-$. Then we have

$$\begin{aligned} e &= b_0 - b_1 + b_2 - b_3 + b_4 \\ &= 1 - b_1 + b^+ + b^- - b_1 + 1 \\ &= 2 - 2b_1 + b^+ + b^-. \end{aligned} \tag{6.1.6}$$

From the above identities we get

$$\begin{aligned} e + \sigma &= (2 - 2b_1 + b^+ + b^-) + (b^+ - b^-) \\ &= 2 - 2b_1 + 2b^+. \end{aligned} \tag{6.1.7}$$

Combining the inequalities (6.1.4) and (6.1.5) gives

$$\begin{aligned} e + \sigma &= (4 - 4g + n + s) + \sigma \\ &\leq (4 - 4g + n + s) + n - s - 4g + 2b_1 \\ &\leq 4 - 8g + 2n + 2b_1. \end{aligned} \tag{6.1.8}$$

Finally, combining (6.1.7) and (6.1.8) gives

$$\begin{aligned} & 2 - 2b_1 + 2b^+ \leq 4 - 8g + 2n + 2b_1 \\ \iff\ & 8g - 4b_1 + 2b^+ - 2 \leq 2n \\ \iff\ & 4g - 2b_1 + b^+ - 1 \leq n\,, \end{aligned} \tag{6.1.9}$$

which is the first inequality in the statement.

The second inequality follows from the following observations: The collection of s vanishing cycles yield s disjoint surfaces of self-intersection (-1). Moreover, the homology class of the regular fiber F is in the orthogonal complement (with respect to the intersection form) of the subspace of $H_2(X;\mathbb{Q})$ generated by these s surfaces. Note that F is homologically essential: if $g \neq 1$, the first Chern class of any almost complex structure compatible with the fibration evaluates nontrivially on F, and for $g = 1$, our assumption that we have a nontrivial Lefschetz fibration implies that it has a section. Thus, F should have a dual in the orthogonal complement, which contributes one more dimension to the negative eigenspace of the intersection form, in addition to the other s. Then it follows that

$$s \leq b^- - 1. \tag{6.1.10}$$

□

6.2 Signature of the generalized Baykur-Korkmaz Lefschetz fibrations

We calculate the signatures of the generalized Baykur-Korkmaz Lefschetz fibrations here. Note that for this calculation, as well as the one in the next section, we are looking at the Lefschetz *fibrations* (and not pencils).

Lemma 6.2.1. *The signature of the total space of any genus–g Baykur-Korkmaz Lefschetz fibration X_{BK} is*

$$\sigma(X_{\mathrm{BK}}) = -g - 1$$

.

Proof. By Corollary 5.1.4, our genus g Lefschetz fibration X_{BK} has a monodromy factorization lifted from a planar factorization with $4(g-1)$ arc half-twists, yielding

$n_{\mathrm{I}} = 4(g-1)$. In this planar factorization there are g squared odd parity Dehn twists around 3 marked points and one squared odd parity Dehn twist around $2g-1$ marked points, all yielding vanishing cycles bounding a genus one subsurface. Since these are all the contributors to the positive factorization for X_{BK}, we have $n_1 = g+1$ and $n_i = 0$ for $2 \leq i \leq \lfloor g/2 \rfloor$ in the factorization. Thus, by Endo's signature formula we have got:

$$\begin{aligned}
\sigma &= n_{\mathrm{I}}\sigma_g(\mathrm{I}) + n_1\sigma_g(\mathrm{II}_1) \\
&= 4(g-1)\sigma_g(\mathrm{I}) + (g+1)\sigma_g(\mathrm{II}_1) \\
&= \frac{-4(g-1)(g+1)}{2g+1} + (g+1)\left[\frac{4\cdot 1(g-1)}{2g+1} - 1\right] \\
&= \frac{-4(g-1)(g+1) + 4(g-1)(g+1)}{2g+1} - (g+1) \\
&= -g-1.
\end{aligned} \tag{6.2.2}$$

□

6.3 First homology of the generalized Baykur-Korkmaz Lefschetz fibrations

Here we calculate the first homology of the total space X_{BK} for any genus g using (5.2.1) in the previous chapter. We will then conclude that $b_1(X_{\mathrm{BK}}) = 2$.

The Dehn twists in the planar factorizations are all squared with odd parities, so they lift to separating curves with zero homology. For example, the homology classes of the vanishing cycles of the genus–2 Lefschetz fibration X_{BK} (as depicted in Figure 6.1, after capping all boundaries) has three squared twists on the left, t_c^2, t_d^2, and t_e^2, lifting to $t_{\overline{c}}$, $t_{\overline{d}}$, and $t_{\overline{e}}$ on the right. The four remaining arc half-twists in this case lift to four Dehn twists around the curves A_2, B_2, C_2, and E_2. This pattern continues, with each genus $k \geq 2$ X_{BK} consisting of Dehn twists around the same curves as the genus $k-1$ case, Dehn twists around four additional curves A_k, B_k, C_k,

and E_k, and Dehn twists around separating curves which don't contribute to the homology calculation.

Lemma 6.3.1. *For each $g \geq 2$, the homology classes of the vanishing cycles A_k, B_k, C_k and E_k of $f_g \colon X_{\mathrm{BK}} \to S^2$ in $H_1(\Sigma_g; \mathbb{Z})$ are prescribed by the $4(g-1)$ arcs in the $(g-1)$ arc quartets for $2 \leq k \leq g$ as:*

$$\begin{aligned} A_k &= a_1 + a_2 + \cdots + a_k + b_k - b_1, \\ B_k &= 2a_1 + 2a_2 + \cdots + 2a_{k-1} - b_1 + 2b_k, \\ C_k &= a_1 + a_2 + \cdots + a_{k-1} - a_k + b_k, \\ E_k &= 2a_k - b_1 \end{aligned} \tag{6.3.2}$$

where $\{a_i, b_i\}$ is the symplectic basis for $H_1(\Sigma_g; \mathbb{Z})$ given by the curves in Figure 5.1

Proof. The genus 2 case is easily calculated from Figure 6.1 using (5.2.1). Using induction, the genus $g > 2$ case follows from the genus $g-1$ case, considering Figure 6.2. In our chosen homology basis, the vanishing cycles A_k, B_k, C_k, and E_k are disjoint from a_i and b_i whenever $k < i \leq g$, so their homology expressions given in (6.3.2) is unchanged from the genus $g-1$ case. The vanishing cycles A_g, B_g, C_g, and E_g intersect a_i and b_i exactly as $A_{g-1}, B_{g-1}, C_{g-1}$, and E_{g-1} do when $2 \leq i < g$, while they intersect a_g and b_g exactly as a_{g-1} and b_{g-1} intersects $A_{g-1}, B_{g-1}, C_{g-1}$, and E_{g-1}. □

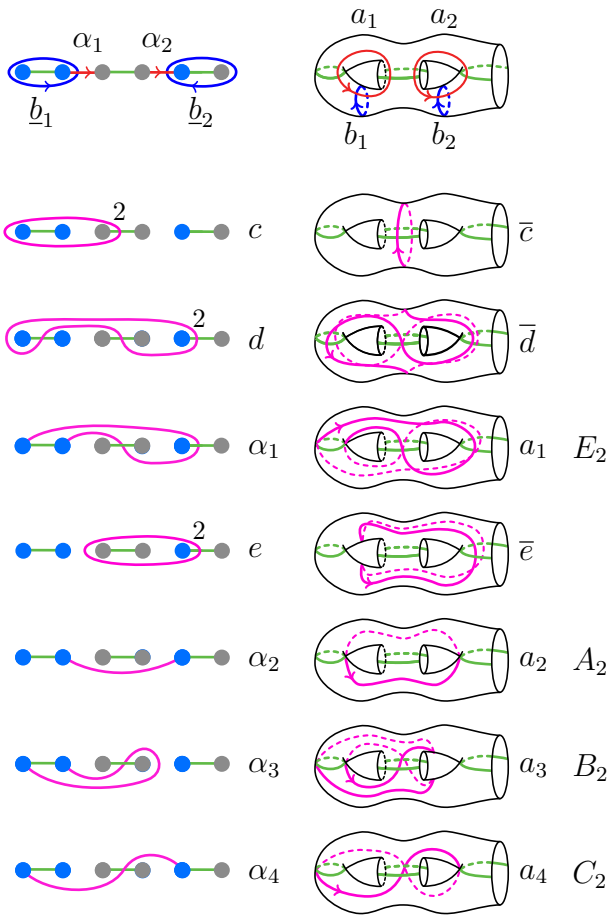

Figure 6.1. Vanishing cycles of the genus–2 Lefschetz fibration X_{BK} with (arbitrary) orientations added to the vanishing cycles to calculate the algebraic intersections.

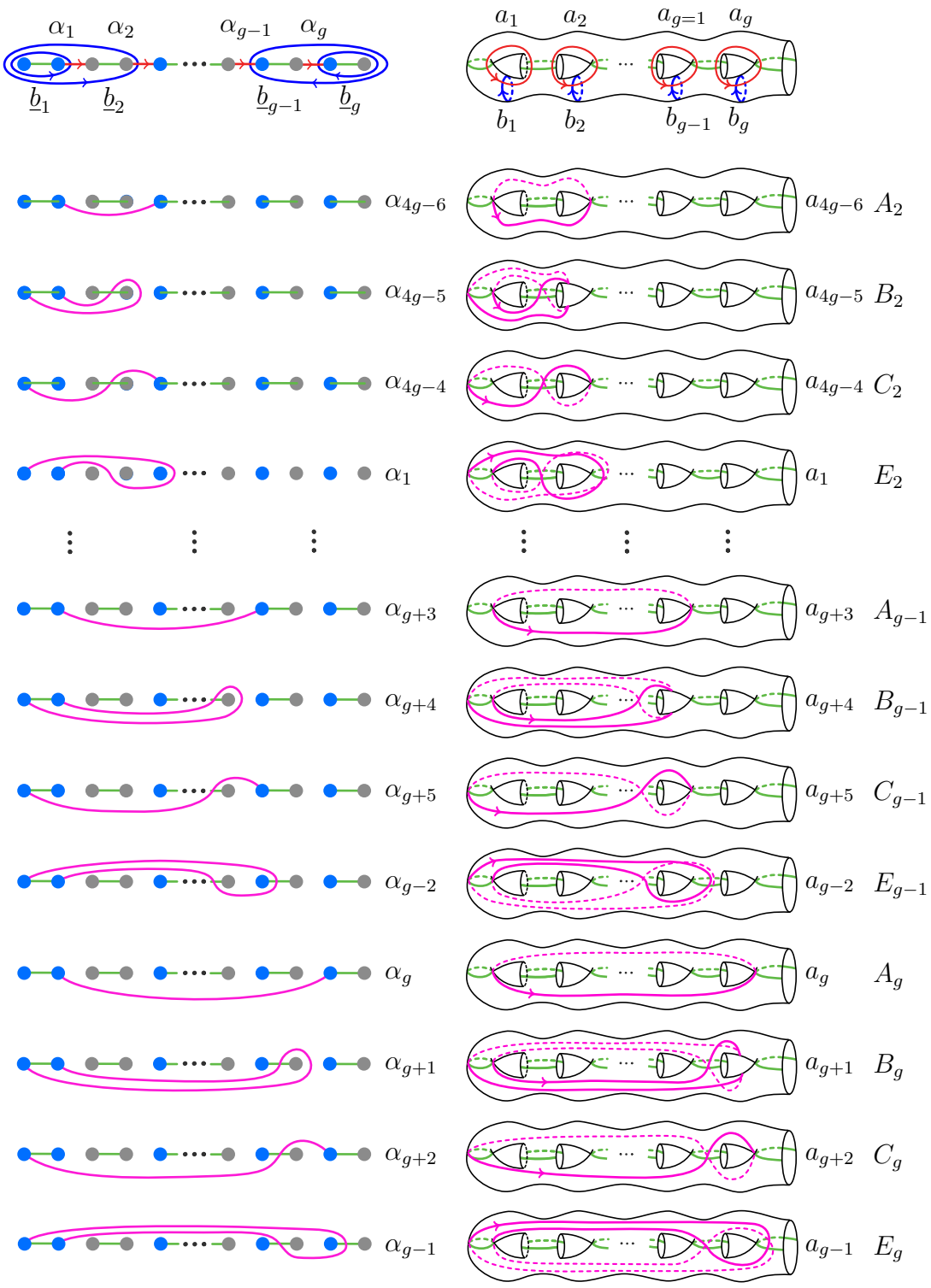

Figure 6.2. Vanishing cycles of the general genus–g Lefschetz fibration X_{BK} with (arbitrary) orientations to calculate the algebraic intersections. Relabeling of the non-separating vanishing cycles as A_k, B_k, C_k and E_k are as shown in the figure.

Lemma 6.3.3. *For all genus g, $H_1(X_{\mathrm{BK}};\mathbb{Z}) \cong \mathbb{Z}^2 \oplus \mathbb{Z}_2^{g-2}$, so $b_1(X_{\mathrm{BK}}) = 2$.*

Proof. Using the above lemma, we express the homology classes of A_k, B_k, C_k, and E_k in terms of the symplectic generators $a_1, b_1, \ldots, a_g, b_g$. Equating each to zero then determines the relations induced in $H_1(\Sigma_g;\mathbb{Z})$, giving us the calculation of $H_1(X_{\mathrm{BK}};\mathbb{Z})$. Note that all these Lefschetz fibrations have sections (easy to see from our derivations) so there is no other relation in $H_1(X_{\mathrm{BK}};\mathbb{Z})$.

The first pair of each quartet is actually given by the second pair, since we have $A_k = C_k + E_k$ and $B_k = 2C_k + E_k$ in $H_1(\Sigma_g;\mathbb{Z})$. For the remaining two, $C_k = 0$ implies that $b_k = a_k - a_{k-1} - \cdots - a_1$, and $E_k = 0$ implies that $b_1 = 2a_k$.

We are better off changing the basis here. [1] For $3 \leq k \leq g$, take $a'_k := a_k - a_{k-1}$ and continue to use a_1, a_2, and $b_1, \ldots, b_g$ in the new basis. Then for each $3 \leq k \leq g$, we have $a_k = a'_k + a_{k-1}$, so that $a_k = a'_k + a'_{k-1} + \cdots + a'_3 + a_2$.

The relations induced by $C_k = 0$ and $E_2 = 0$ now express each b_k in terms of $a_1, a_2, a'_3, \ldots, a'_k$ in $H_1(X_{\mathrm{BK}};\mathbb{Z})$. We can remove all the generators b_k with $k \geq 2$ and the relations induced by C_k while rewriting the relations induced by $E_k = 0$, for $k \geq 2$ as $2a'_k = 0$ (since for each $3 \leq k \leq g$, $2a_k = b_1$). Hence $H_1(X_{\mathrm{BK}};\mathbb{Z}) \cong \mathbb{Z}^2 \oplus \mathbb{Z}_2^{g-2}$. □

6.4 The main theorem

We are ready to prove our main result.

Theorem 6.4.1. *For each $g \geq 2$, the generalized Baykur-Korkmaz genus–g Lefschetz fibration $f_g\colon X_{\mathrm{BK}} \to S^2$ has $b_1 = 2$, $b^+ = 1$, $b^- = g + 2$, and $n = 4(g-1)$ nonseparating vanishing cycles and $s = g + 1$ separating vanishing cycles. It follows that the inequalities* (6.1.2) *and* (6.1.3) *are (simultaneously) sharp.*

Proof. The monodromy factorization for X_{BK} shows that $n = 4(g-1)$ and $s = g+1$. From Lemma 6.3.3, we have $b_1 = 2$.

---

[1] I'm grateful to my advisor İnanç Baykur for suggesting this basis change.

Since there are $\ell = n + s = 5g - 3$ vanishing cycles, we get

$$\begin{aligned} e &= 4 - 4g + \ell \\ &= 4 - 4g + (5g - 3) \\ &= g + 1. \end{aligned} \tag{6.4.2}$$

Using equation (6.1.6), we get

$$\begin{aligned} 2 - 2b_1 + b^+ + b^- &= g + 1 \\ \iff b^+ + b^- &= g + 3. \end{aligned} \tag{6.4.3}$$

On the other hand, as we have $\sigma = -g - 1$ by Lemma 6.2.1, we also conclude that

$$b^+ - b^- = -g - 1. \tag{6.4.4}$$

Combining the equalities (6.4.3) and (6.4.4), we conclude that $b^+ = 1$ and $b^- = g + 2$

Hence, the inequalities (6.1.2) and (6.1.3) for these examples would read:

$$n \geq 4g - 2b_1 + b_2^+ - 1 = 4g - 4$$

and

$$s \leq b^- - 1 = g + 1\,,$$

which are sharp for $n = 4g - 4$ and $s = g + 1$. □

We should note that, unlike most inequalities involving the invariants of Lefschetz fibrations in the literature, the proofs of the above basic inequalities (6.1.2) and (6.1.3) do not use any arguments coming from gauge theory or symplectic geometry, but rely only on elementary arguments from handlebody theory and algebraic topology, which

makes it all the more surprising that these inequalities are in fact sharp. Even more, the sharp examples come from the more restricted family of hyperelliptic Lefschetz fibrations!

BIBLIOGRAPHY

[Bay22] R. İnanç Baykur, *Small exotic 4-manifolds and symplectic Calabi-Yau surfaces via genus-3 pencils*, Gauge theory and low-dimensional topology—progress and interaction, 2022, pp. 185–221. MR4600724

[BH] R. İnanç Baykur and N. Hamada, *An exotic symplectic rational surface*, In preparation.

[BK17] R. İnanç Baykur and Mustafa Korkmaz, *Small Lefschetz fibrations and exotic 4-manifolds*, Math. Ann. **367** (2017), no. 3-4, 1333–1361. MR3623227

[Cad98] Carlos Alberto Cadavid, *On a remarkable set of words in the mapping class group*, ProQuest LLC, Ann Arbor, MI, 1998. Thesis (Ph.D.)–The University of Texas at Austin. MR2699379

[Don99] S. K. Donaldson, *Lefschetz pencils on symplectic manifolds*, J. Differential Geom. **53** (1999), no. 2, 205–236. MR1802722

[EMVHM11] Hisaaki Endo, Thomas E. Mark, and Jeremy Van Horn-Morris, *Monodromy substitutions and rational blowdowns*, J. Topol. **4** (2011), no. 1, 227–253. MR2783383

[EN05] Hisaaki Endo and Seiji Nagami, *Signature of relations in mapping class groups and non-holomorphic Lefschetz fibrations*, Trans. Amer. Math. Soc. **357** (2005), no. 8, 3179–3199. MR2135741

[End00] Hisaaki Endo, *Meyer's signature cocycle and hyperelliptic fibrations*, Math. Ann. **316** (2000), no. 2, 237–257. MR1741270

[FM12] Benson Farb and Dan Margalit, *A primer on mapping class groups*, Princeton Mathematical Series, vol. 49, Princeton University Press, Princeton, NJ, 2012. MR2850125

[GS99] Robert E. Gompf and András I. Stipsicz, *4-manifolds and Kirby calculus*, Graduate Studies in Mathematics, vol. 20, American Mathematical Society, Providence, RI, 1999. MR1707327

[Kas80] A. Kas, *On the handlebody decomposition associated to a Lefschetz fibration*, Pacific J. Math. **89** (1980), no. 1, 89–104. MR596919

[MW21] Dan Margalit and Rebecca R. Winarski, *Braids groups and mapping class groups: the Birman-Hilden theory*, Bull. Lond. Math. Soc. **53** (2021), no. 3, 643–659. MR4275077

[PVHM10] Olga Plamenevskaya and Jeremy Van Horn-Morris, *Planar open books, monodromy factorizations and symplectic fillings*, Geom. Topol. **14** (2010), no. 4, 2077–2101. MR2740642

[Sta62] John Stallings, *The piecewise-linear structure of Euclidean space*, Proc. Cambridge Philos. Soc. **58** (1962), 481–488. MR149457